WELLBORE INSTABILITY ANALYSIS FROM A HIGHLY FRACTURED CARBONATE GAS RESERVOIRS

BY

ABDULRAHMAN MOHAMMED AL-NUTAIFI

A Thesis Presented to the

DEANSHIP OF GRADUATE STUDIES

KING FAHD UNIVERSITY OF PETROLEUM & MINERALS

DHAHRAN, SAUDI ARABIA

In Partial Fulfillment of the
Requirements for the Degree of

MASTER OF SCIENCE

In

PETROLEUM ENGINEERING

January 2019

KING FAHD UNIVERSITY OF PETROLEUM & MINERALS

DHAHRAN- 31261, SAUDI ARABIA

DEANSHIP OF GRADUATE STUDIES

This thesis, written by **AbdulRahman Mohammed Al-Nutaifi** under the direction of his thesis advisor and approved by his thesis committee, has been presented and accepted by the Dean of Graduate Studies, in partial fulfillment of the requirements for the degree of **MASTER OF SCIENCE IN PETROLEUM ENGINEERING.**

Dr. Abdulazeez Abdulraheem
(Thesis Advisor)

Dr. Dhafer A. Al-Shehri
Department Chairman

Dr. Mohammed Mahmoud
(Member)

Dr. Salam A. Zummo
Dean of Graduate Studies

9/4/19
Date

Dr. Salaheldin Elkatatny
(Member)

DEDICATION

This work is dedicated to my much-beloved parents, my wife and my young boys Mohammad and Faisal.

ACKNOWLEDGMENTS

I would like to thank my thesis advisor, Dr. Abdulazeez Abdulraheem for his support and encouragement to achieve and complete the thesis requirements. I also appreciate Dr. Mandefro Woldeamanuel from Saudi Aramco for his support and guidance before, during and after completing my thesis. I am also grateful to the thesis committee members, Dr. Mohammed Nasser and Dr. SalahEdin El-Katatny for their continuous support. I am also thankful to my colleagues Meshal Al-Amry and Hamad Al-Kharra for their support during the thesis work. I would like also to extend my deep appreciation to Dr. Antonio Santagati and Mr. Edwin Caliboso from Saudi Aramco's EXPEC Advanced Research Center for their support during the rock mechanical testing experiments included in the thesis work.

I highly appreciate Saudi Aramco managements support for their permission to publish this work. I am also thankful for the Petroleum Engineering Department and the Deanship of Graduate Studies at King Fahd University of Petroleum & Minerals for their continuous support in allowing extensions to ensure the completion of the thesis work.

TABLE OF CONTENTS

LIST OF FIGURES

LIST OF TABLES

LIST OF ABBREVIATIONS

σ	:	Total Stress, psi
ν	:	Poisson's Ratio
Estat	:	Static Young's Modulus, psi
E_{dyn}	:	Dynamic Young's modulus, psi
ν_{dyn}	:	Dynamic Psion's ratio
Vstat	:	Static Psion's ratio
σ_v	:	Vertical (overburden) stress, psi
Δt	:	Sonic slowness, us/ft
ε_x	:	Cartesian (principle) horizontal strains, ft
σ_{Hmin}	:	Minimum horizontal principal stress, psi
σ_{Hmax}	:	Maximum horizontal principal stress, psi
DTCO	:	Compression slowness.
DSTM	:	Shear slowness.
G	:	Shear Modulus, Mpsi
g	:	Gravitational Acceleratio Constant
GR	:	Gamma Ray, unit of API
K	:	Bulk Modulus
LCM	:	Lost Circulation Material

MEM	:	Mechanical Earth Model
MW	:	Mud weight, ppg
Φ	:	Porosity, %
Pp	:	Pore pressure, psi
τ	:	Shear stress
UCS	:	Unconfined Compressive Strength, psi
YM	:	Young's Modulus, GPa
P	:	Density, g/cm^3
MDT	:	Modular Dynamic Tester
DST	:	Drill Stem Test
FIT	:	Formation Integrity Test

ABSTRACT

Full Name : AbdulRahman Mohammed A. Al-Nutaifi

Thesis Title **"**Wellbore Instability Analysis in a Highly-Fractured Carbonate Gas Reservoirs"

Major Field : Petroleum Engineering

Date of Degree : January 2019

Wellbore instability problems are one of the major challenges facing the oil and gas drilling operations impacting drilling efficiency, hindering its progress and potentially leading to damaging the wellbore. Those problems are consequence of violating the balance between the wellbore fluid pressure "mud weight" and the formation pressure "earth stress". Not having such balance can result in undesired problems that varies from loss circulations to stuck pipes or tools that may jeopardize well integrity and result in a total loss of wells and assets. These problematic situations are even worse in fractured reservoir environments where highly fracture zones are mechanically weekend and the probability of wellbore instability increases while drilling through such zones. Considering the high cost of drilling operations, analyzing such problems are critical for companies especially developing fields in harsh drilling environments such as offshore, deep water or remote locations. A one day lost time might result in loss of millions USD of drilling cost in addition to supplying materials and equipment needed to control the wellbore instability.

The problem addressed in this thesis work is based on actual drilling challenges experienced in developing a naturally fractured carbonate reservoir. The development plan was to drill vertical and slightly deviated wells. During early phase of the field development, sever loss circulation were encountered that resulted in lost drilling times estimated in millions of US dollars with rig cost up $ 200,000 Per Day. Other drilling failures include, stuck drill pipe and difficulties associated with logging and logs interpretation.

The study's objective is to investigate the wellbore instability events during drilling operations and explain them as a function of rock properties and in-situ earth stress. The role of natural fractures will be highlighted using available data. There are various subsurface and surface data which were collected and integrated to determine the main reasons behind the loss circulation problems. These available data included drilling parameters, logging, core, image logs and well testing data. Detailed rock mechanics lab tests were carried on available core plugs during the thesis work to improve simulation models used in this study. Integration of these data streams through the construction of Mechanical Earth Models is to develop a better understanding of reasons behind loss circulation. In addition, existing static, dynamic and drilling data will be analyzed in order to potentially find ways to predict the loss circulation events and recommend modification for future drilling programs as well as future development of the field.

ملخص الرسالة

الاسم الكامل: عبد الرحمن محمد عبدالله النتيفي

عنوان الرسالة: تقييم عدم الاستقرار خلال حفر ابار مكامن الغاز الكربونية ذات التصدع العالي

التخصص: هندسة بترول

تاريخ الدرجة العلمية: يناير 2019

أحد أهم التحديات الرئيسية التي تواجه عمليات الحفر لإنتاج النفط والغاز هي تخفيف أثر عدم استقرار المكامن خلال عمليات حفر الابار. ينتج عدم الاستقرار خلال عمليات الحفر من عدم تساوي ضغط سوائل الحفر وضغط المكامن. عدم الاستقرار قد يسبب مشاكل عدة من فقدان سوائل الحفر الى ان تصل إلى وجود أنابيب عالقة قد تعرض سلامة البئر للخطر وربما تؤدي إلى فقدان تام للآبار. هذه الحالات أكثر تعقيدا في بيئات المكامن ذات التصدع العالي حيث تكون تحديد مواقع التصدع امر مهم. تحليل مثل هذه المشاكل أمر بالغ الأهمية بالنسبة للشركات وخاصة في تطوير الحقول البحرية حيث ان خسارة يوم واحد لمعالجة هذه المشاكل قد يؤدي إلى خسارة ملايين الدولارات. وهناك عدة طرق لتحديد العامل الرئيس خلف هذه المشاكل من عينات المكامن ونتائج الاختبارات التي تتم على الابار. ولقد ظهر مجال ميكانيكا الصخور لربط تلك الظواهر إلى خواص مكامن الصخور ودرجات الإجهاد الخاص بها. دمج هذه التقنيات مع تحليل مكثف للمعلومات التي تم جمعها خلال حفر الابار والتي أيضا يمكن جمعها من عينات الصخور والاختبار الأساسية يساهم في فهم الأسباب الكامنة وراء هذه المشاكل وتوفير الحلول لها.

محور هذه الرسالة هو مكمن ذو صخور كربونية. وتم تطوير هذا الحقل من خلال الحفر الرأسي، والحفر المائل. خلال عمليات التطوير، تسبب فقدان سوائل الحفر الشديدة الى خسائر تقدر بملايين الدولارات الأمريكية بتكلفة تصل الى 200،000 $ في اليوم. صعوبات الحفر الأخرى تشمل، أنابيب الحفر العالقة والصعوبات مع تسجيل لتفسير اختبارات الابار.

الهدف من هذه الدراسة هو التحقيق في عدم الاستقرار أثناء عمليات الحفر من خلال تحليل خواص الصخور الميكانيكية والإجهاد الأرض تحت ظروف المكمن. سيتم تسليط الضوء التركيز على دور الكسور الطبيعية والمدرجة في نماذج المدخلات من خلال المعطيات المتوفرة. أثناء الدراسة، سيتم تحليل بيانات معلومات الآبار الموجودة في الحقل ونتائج المسح الجيولوجي لوضع تصور عن كيفية التنبؤ بالمواقع التي ممكن ان تحدث مثل هذه المشاكل فيها في المستقبل. وبناء على هذه النتائج سيتم اتخاذ توصيات للآبار الحفر المستقبلية لتفادي مثل هذه المشاكل المصاحبة لعمليات الحفر.

CHAPTER 1

INTRODUCTION

Historically, drilling operation technologies and practices went through various phases and major advancements. The introduction of deviated and horizontal wells opened new horizons for accessing restricted sub-surface reservoirs and areas. However, it also introduced challenges encountered related to wellbore instability. The Borehole instability history can be divided into two parts: (1) Pre-horizontal drilling, which spanned a long time since the first oil well was drilled by Drake (1858) and (2) Post-horizontal drilling, which became a routine drilling paradigm since the 1980's. Figure 1 shows summary of wellbore instability phases evolution (eras) through the history of drilling operations.

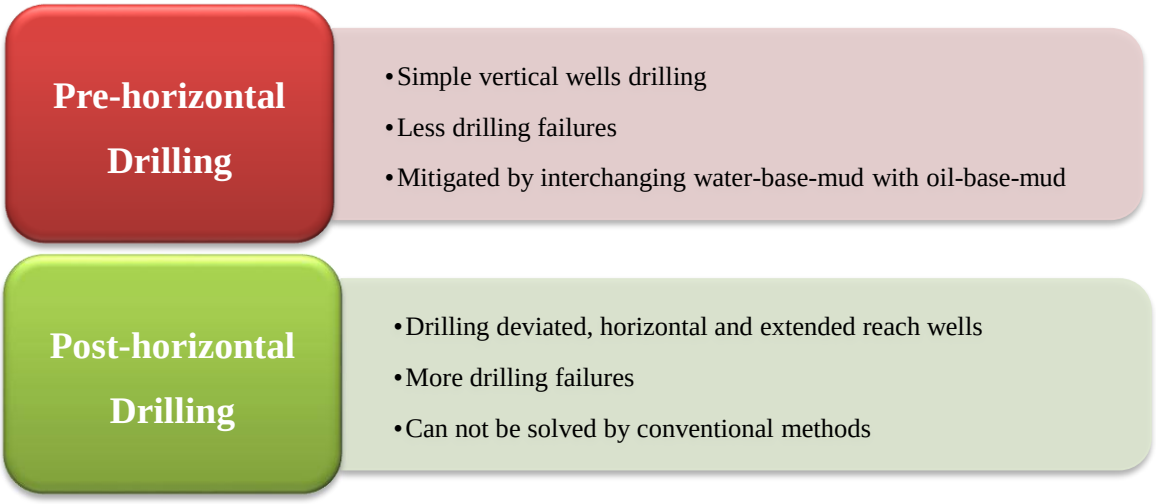

Figure 1: Classification of borehole instability eras

Consequently, with the advent of new drilling approaches, a new class of drilling instability problems emerged, which were initially mitigated with controlling the factors that were

supposed to impact the wellbore stability during drilling operations which will be discussed later in this chapter.

1.1 Wellbore Stability

Wellbore stability while drilling operations is controlled by the stress-state around the wellbore and the rock's strength. As the drill bit cuts into the formations, it replaces cylindrical volume of rock material with equivalent volume of drilling fluid "mud". The drilling fluid weight is "usually referred to as mud weight" is the support against the formation. There are several terminologies associated with the understanding of interaction between drilling fluid mud weight and reservoir rock properties which are listed below.

- **Pore pressure** is the pressure of the fluids within the pores of the reservoir, usually hydrostatic pressure or the pressure of the water column from the formation's depth to the sea level.
- **Fracture gradient pressure** is the pressure required to open an existing fractures in the formation rock at given depth.

Those pressure points control the safe mud weight operating window. The safe mud weight window is defined as the limits (maximum and minimum mud weight) needed to avoid wellbore instability. Exceeding this window with heavy mud-weight (i.e. exceeding the fracture gradients) creates loss circulations issues "Tensile Failures". On the other hand, operating at mud weight less than formation collapse pressure "Compressive Failures".

Compressive failures are caused by an insufficient mud weight compared with the rock's strength and the stresses around the wellbore. Compressive failures can be divided into two main types: (1) an increased wellbore diameter due to brittle failure and the subsequent caving in of the wellbore wall. This phenomenon occurs in brittle rocks in general, and can lead to cementing problems and difficulties with logging response and log interpretation, and (2) a reduced wellbore diameter which occurs in weak (plastic) sandstones and salts. This phenomenon requires repeated reaming or may even result in a stuck drill pipe.

Tensile failure is caused by an excessive mud weight compared with the minimum in-situ stress. The higher the mud weight make the hydrostatic pressure exceed the fracture gradient which create paths for fluid to penetrate the reservoir. This is recognized by lost circulation of drilling fluid. This can reduce the hydraulic pressure in the well and cause an inflow of the pore fluid. To control the drilling parameters, mainly mud weight, the industry adopted the concept of the safe mud weight window where the upper and lower allowable limits of the mud weights are defined from both pore pressure and fracture gradients. Figure 2 shows different regions in the mud weight window and their interpretations.

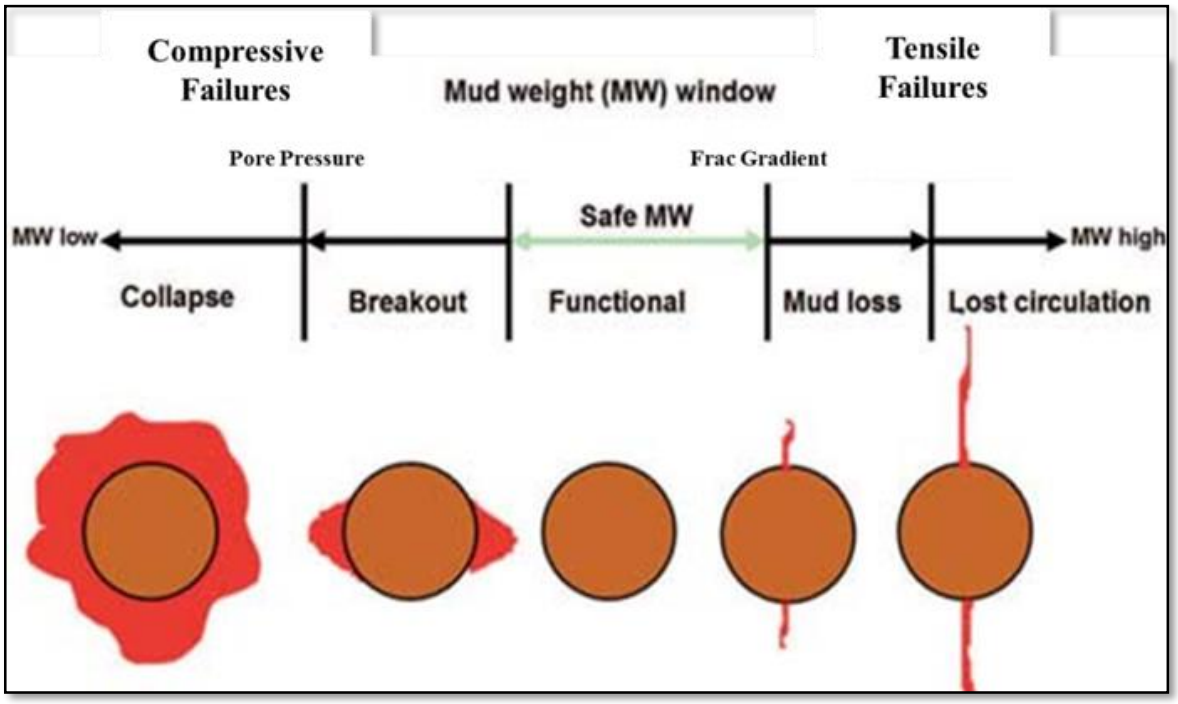

Figure 2: Mud-weight windows and associated failures (Zoback, 2007)

The regions in Figure 2 can be summarized as follows:

- **Well Collapse:** where the well losses its integrity and rock fails due to having the mud weight equivalent pressure is less than pore pressure. Breakout can be used to map the direction of SHmin.
- **Well Breakout:** where the well partially fails in the area near the wellbore due to having the mud weight equivalent pressure is close to the pore pressure. Breakout can be used to map the direction of minimum horizontal stress.

- **Mud Losses:** where the mud weight equivalent pressure is close the fracturing gradient enabling the fluid to seep through the weakest reservoir while maintaining wellbore circulation.
- **Lost Circulation:** where the mud weight equivalent pressure is higher than the fracturing gradient creating drilling, induced tensile fractures increasing preventing wellbore circulation.

The factors behind wellbore instability can be classified into two type's controllable and incontrollable factors. Controllable factors are well trajectory (vertical vs. horizontal), drilling parameters type of mud (water base or oil base), mud weight and flow rate, downhole temperatures and completion/ treatment choices. On the other hand, there parameters that cannot be controlled or altered are rock strength, rock mechanical properties and in-situ stresses.

The field of rock mechanics emerged to connect wellbore instability to some of the uncontrollable drilling factors such as reservoir rock properties and stress profiles. This will help in constructing completion and drilling programs that avoids the wellbore instability issues based on the cumulative knowledge from previous drilling operations.

Moreover, coupling the study of rock mechanics with an intensive analysis of drilling reports, new logging technologies, advanced core testing and other data attributes builds a framework that helps in understanding the roots behind those failures and introduce proactive measures to avoid them in the future drilling operations.

1.2 Earth Stresses

There are three principal stress component (tensors) which defines the stress orientations and magnitudes at any point in the earth. These are namely, Vertical or overburden stress (σ_v), Maximum Horizontal Principal Stress (σ_{Hmax}) and Minimum Horizontal Principal stress (σ_{Hmin}). The three principal stresses are orthogonal as shown in the Figure 3. When drilling the wellbore, we are replacing a cylinder of rock with cylinder of fluid of different density. The rock can support both shear and normal stresses but the mud is unable to support shear stress. This leads to distribution of the in-situ stress, which was once in equilibrium, which can be strong enough to make the rock deform or fail.

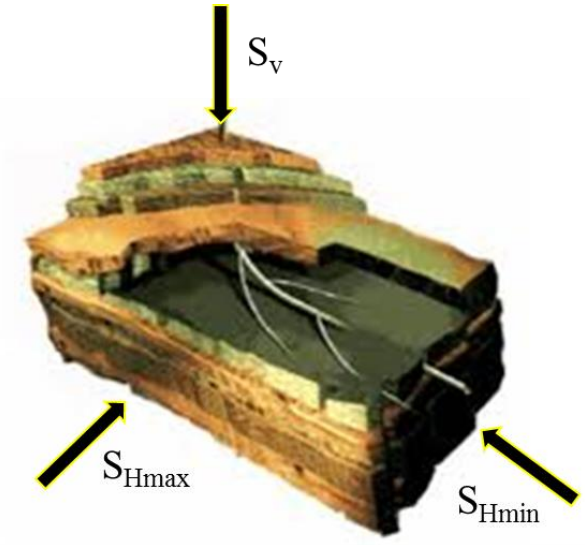

Figure 3: The three earth principal stresses

However, if the rock is fractured, it is mechanically weakened and exhibits high-permeability fluid-flow stream within considerably less permeability intact reservoir matrix. Because of different fluid-flow rates between the fracture network and intact matrix, there are two distinct pore-pressure when subjected to stress. For example, in overbalanced drilling through a fractured formation, the drilling mud penetrates the fractures immediately and there is no significant leak-off of fluid from the wellbore or from the fractures into the intact matrix. In other words, the fracture network with high permeability provides preferential flow paths for mud invasion into the formation. Consequently, the risk of losing mud circulation and damaging the formation is much higher. In addition, the fluid invasion into the fractures weakens the mechanical strength of the formation. Furthermore, the communication between the fluid pressure in the fractures and wellbore mud pressure makes the formation more sensitive to every activity in the drilling operation such as stopping circulation, tripping, or drill string impact.

1.3 Statement of the Problem

The study area is developed by drilling vertical and deviated wells in naturally fractured environment identified from core and well test data. During drilling activities, wells showed highly problematic wellbore instability in the form of sever loss circulations in multiple events in a single well. This has resulted in huge lost drilling time and in some cases total well loss. An investigation of the root cases for the lost circulation events is required to prevent such events from reoccurring in upcoming drilling activities. Knowledge of rock mechanical properties around the wellbore, the stress state in the field and understanding natural fracture required to help in the analysis.

1.4 Research Objectives

In order to determine the root causes behind the loss circulation experienced in the field of study, a thorough evaluation and analysis of the available data need to be conducted. The objectives to be accomplished through the various phases of the study include the following;

- Gathering and reviewing existing data from wells.
- Conducting Rack Mechanical testing for the available core plugs.
- Modeling of rock mechanical static and dynamic properties.
- Calibration of rock mechanical properties using available core data.
- Construct single well Mechanical Earth Models for selected wells.
- Characterization of Natural fractures using available image logs data.
- Identify root causes for wellbore instability events in drilled wells.
- Predict the wellbore instability for future drilling programs.

1.5 Research Methodology

This study has three different phases. Phase I includes collecting data required for the analysis from existing wells and conducting the quality check and preparation for data utilization needed in upcoming phases. In Phase II, I will construct a geomechanical model using existing data from wells previously drilled in this field. This phase will require analysis of wireline logs, downhole measurements, drilling experiences, and characterization of drilling-induced wellbore failures such as stress-induced borehole

breakouts and drilling induced tensile fractures, through analysis and interpretation of available borehole image and caliper data. I will determine the full stress tensor as a function of depth using a priori values of the least principal stress, overburden, and pore pressure to constrain the magnitude of the maximum principal horizontal stress (σ_{Hmax}) consistent with the observed wellbore failure. The MEM model will be calibrated and verified against core rock mechanical properties measured on collected core plugs to ensure it is sufficiently robust. In Phase III, I will utilize this geo-mechanical model, coupled with available image logs to justify for borehole instability issues encountered and give recommendation for future drilling programs. Additionally, available data will be utilized to correlate the wellbore instability parameters with other rock properties to help predicting the wellbore instability for future drilling program. Figure 4 shows the methodology of the research which will be conducted in this study.

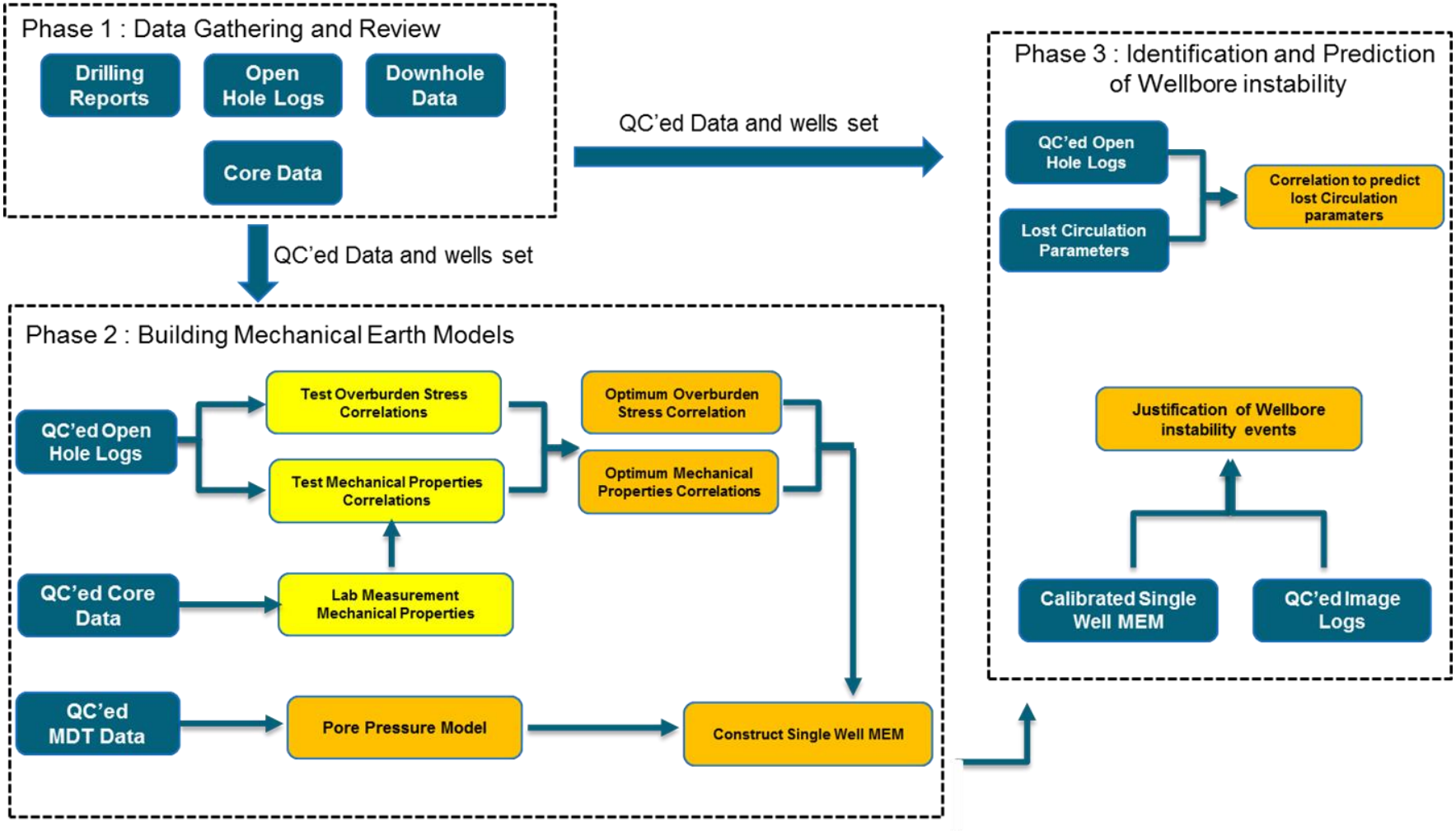

Figure 4: Research Methodology conducted in this study

CHAPTER 2

LITERATURE REVIEW

2.1 Wellbore Instability Problems

Reservoir rock's mechanical properties and stress state around the wellbore were among the primary areas investigated by researchers to describe the wellbore instability problems. Muary [1987] showed the importance of history analysis to identify the different types of drilling problems related to poor borehole behavior and characterized the conditions for occurrence that is in agreement with geo-mechanical behavior of the borehole. They showed that several independent or interconnected factors are controlling the borehole stability: high or low, isotropic or anisotropic horizontal stresses, particular rock rheological behavior, excessive wall stresses induced by fast in and out of well tripping, pressure gradient around the borehole.

Chatterjee et.al [2001] studied the petro physical and mechanical properties of reservoir rocks from two major basins on the east coast of India using core samples from 19 wells. The purpose of the study was to investigate the relationships between the properties of the rocks including dry density, effective porosity, uniaxial compressive strength, tensile strength, and Young's modulus and wellbore failures. Al Burial and Pasnak [1993] discussed the well plans, drilling fluids, casing, cementing liners, coring, logging, completions and drilling problems encountered in more than a dozen horizontal wells drilled both in sandstone and carbonate reservoirs in Saudi Arabia. The wells suffered from

major 13 wellbore instability problems like borehole collapse leading to stuck pipe due to mechanical instability of shale. Several stuck liners and casings were experienced in holes drilled with motor. Kumar et.al [2012] showed case studies from Mumba High North Indian offshore field where loss circulation was sever and increased with directional drilling activity and reservoir depletion as well as other wellbore instability issues. In their study, they outlined detailed procedure to incorporate drilling parameters as well as rock mechanical properties to discuss the encountered issues. With the aid of computer-based algorithms and simulators, it was easier to utilize the rock mechanical properties and cross-link it to the wellbore instability problems.

In the early days, the industry has relied on the simple regression technique to calibrate log derived mechanical properties with static measurements. Al-Mahtani and Rahim [2001] presented a mathematical algorithm for modeling geo-mechanical rock properties of the AA and Pre-AA reservoirs in Gnawer field. The algorithm consists of calibrating the dynamic Young's modulus and Poisson's ratio with static values, evaluating the minimum horizontal stress using the calibrated parameter and then calibrating the evaluated minimum horizontal stress with history matched results. They have also presented three case studies in which they applied the above-mentioned algorithm.

Elissa and Kasi [1988] studied different statistical relations between static and dynamic Young's modulus of the rock. They observed that the linear relationship, which is commonly used in the literature, gives a low coefficient of correlation. They presented a better estimate of the static Young's modulus obtained from an empirical relation between

the logarithm of static Young's modulus and the logarithm of the product of dynamic Young's modulus and density.

2.2 Drilling Fluid Loss Circulation

During the past years, studies were carried out to predict and control the lost circulation of fractured zones plugged with lost circulation material (LCM). Whereas, the stability and strength of the plugged zones have not been reported in such researches which might cause costly drilling operation due to uncured losses triggered by difficulty and complexity of loss-zone diagnosis. Therefore, couple of models, in this area, studies the impact of LCM particles size distribution of these granules for plugging and sealing efficiency improvements. These models include: The Abrams model (1977), ideal-packing theory (Dick et al., 2000), and the Vickers model (Vickers et al., 2010). They all concluded that optimized granule size to plug loss circulation zones is function of the loss-zone geometry (i.e., the median granule size should be equal to one-third of the fracture width). In addition, plugging strength and stability are also impacted by the LCM texture, type and utilized particles' sizes which affect the plugging effectiveness. Furthermore, the formation and fluid crushing and shear stresses affect the strength of the plugged zone effectiveness, which should be enough to sustain such forces.

(Cheng-yuan Xu et al., 2014) conducted a laboratory work to investigate the high-strength and high stability system for minimal loss circulation. In his study, he developed high-strength and high stability pill system while considering rigid particles, fiber, and resilient particles to improve plugging efficiency of the drilling fluid as well as the plugged zone stability. He concluded that the main parameters in affecting plugging stability and capacity

are the volume faction into the plugged zone and surface friction coefficient. His experimental work showed that the high plugging pressure of 15.5 MPa resulted in a total loss volume before sealing to a reduced volume of 50 cm^3 which as a result he was able to obtain a physical model of plugged zone stability with respect to both theoretical and laboratory work.

The compressional-hoop stress formed nearby a naturally fractured wellbore, which defines the stress window, existed and was acknowledged in the literature for analytical approaches of hydraulic fracture studies using material-caging and stress-clamping terminologies (Warren, 1982).

On the other hand, the stress cage theory has been weakened by (Van Oost et al., 2008, Van Oost, et al., 2011 and van Oost and Rizvi, 2014), who observed the relationship between the hoop-stress improvement and wellbore stability and found it questionable. Therefore, lost circulation treatments have been quantified by comparing the leak-off test pre and post curing which indicated an increase in the fracture propagation resistance not its initiation resistance, which contradicts the findings in the stress cage theory.

2.3 Failure Criteria and Wellbore Instability Models

A wide range of modeling approaches are available for assessing borehole instability risks most commonly elastic and poro-elastic models. Elastic model is probably the simplest and work widely used model to describe earth stresses acting on the wellbore. Its components include, vertical “overburden” stress, the two orthogonal horizontal stresses

(maximum and minimum) and the drilling wellbore fluid's hydrostatic pressure. Bradley [1979] was the first to introduce usage of elastic model in wellbore instability that identified the distribution of the stresses in the wellbore. Li et.al [1988] used the elastic model developed by Bradley to study the fracturing propagation planes through construction of 3D stress models. Mclean and Addis [1990] included other failure criteria effects on the elastic wellbore instability model, which showed huge impact on the calculation of the safe mud weight window. Zhou et.al [1996] investigated the impact of wellbore orientation on stress distribution in which he concluded that selecting the optimal inclination angle would minimize wellbore instability risk.

Poro-Elastic Horizontal Strain Model is the most generally used method for horizontal stresses calculation. The Poro-Elastic Horizontal Strain Model can be expressed using Static Young's modulus, Poisson ratio, Biot's constant, overburden stress, and pore pressure. Biot [1941] developed the poro-elastic model to study the reservoir rock consolidation. More recent evaluations and utilization of the poro-elastic theory was carried by Cui et.al [1998] and Hodge et.al [2006] to investigate the impact of time-dependent parameters on the stress state around the wellbore. Santarelli and Brown [1987] developed a poro-elastic model as function of pressure dependent properties. Yamamoto et.al [2006] constructed 3D poro-elastic model for studying wellbore instability in shales in Japan. He showed that extensions of elastic models include the calculation of the borehole breakout angle, the effects of weak bedding planes on rock failure and localized pore pressure and shear stress peaks occurring away from the borehole wall. Linear elastic models are popular because they are relatively easy to implement, require a modest number

of input parameters, and are capable of assessing borehole instability risks for most well trajectories.

Jaeger et.al [1979] first introduced the Mohr-Coulomb Stress Model after combining the work of Mohr and coulomb. It was described as a failure model that gives a relationship between two principal stresses if the formation is at failure. The model assumes that the maximum in-situ shear stress is governed by the shear strength of the formation, which is characterized by the Mohr-Coulomb failure criterion shown in Figure 5. The model is not limited to any specific deformation mechanism or principal stress direction. Therefore, it can be applied to sedimentary basins subjected to either active tectonic compression or extension. Assuming that the vertical stress is a principal stress, the limits of horizontal stresses in the stress domain are the lower limit of minimum horizontal stress, and the upper limit of maximum horizontal stress which are both are estimated from the Mohr-Coulomb Stress Model.

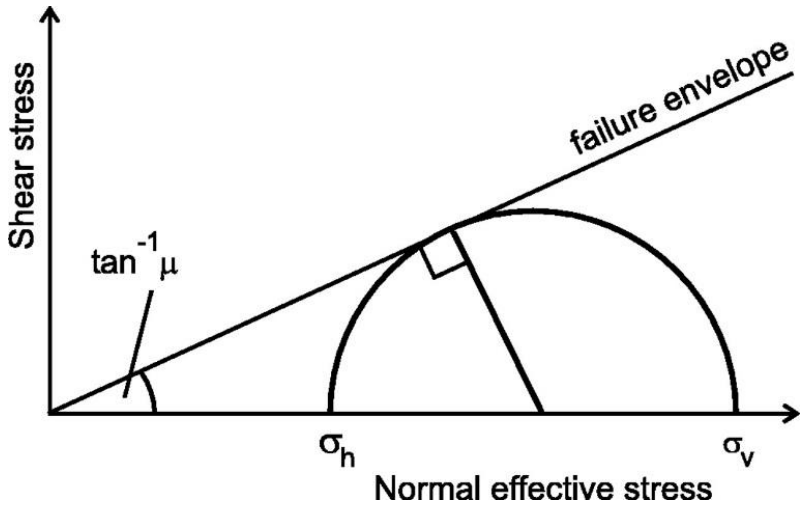

Figure 5: Mohr Circle and related Stresses as function of Normal and Shear Stresses after McLean [2004]

Last et.al [1995] integrated the work from Plumb and Mclean year to describe a new integrated approach of constructing Mechanical Earth Model (MEM) as a numerical integration of rock mechanical properties with the stress state around the wellbore to predict wellbore instability. Important component of the MEM is relating the dynamic acoustic log-based properties to static data measured in the laboratory testing. Estimating the elastic properties of the formation in both static and dynamic is critical for the construction of the Mechanical Earth Model (MEM). The highlighted MEM need to encompass properties such as Young's modulus (E), Possion ratio (v), Biot coefficient (α) Unconfined Compressive Strength (UCS), and Friction Angle (F.A.). There are several correlations available in the literature to estimate those properties in the absence of reliable core data.

The Young's modulus (E) describes the relationship between the stress "pressure" applied on an object and its deformation "strain" all measured in single direction (axial). It is evaluated as the slope of the linear portion of the stress strain relationship for a given confining pressure as indicated in Figure 6 and equation 2.1. (Zoback, 2007).

$$E = \frac{(\text{axial stress})}{(\text{axial strain})} = \frac{\Delta\sigma}{\Delta\varepsilon} \qquad (2.1)$$

Where, σ is the applied stress, Psi,

ε is the strain in the direction of the applied stress.

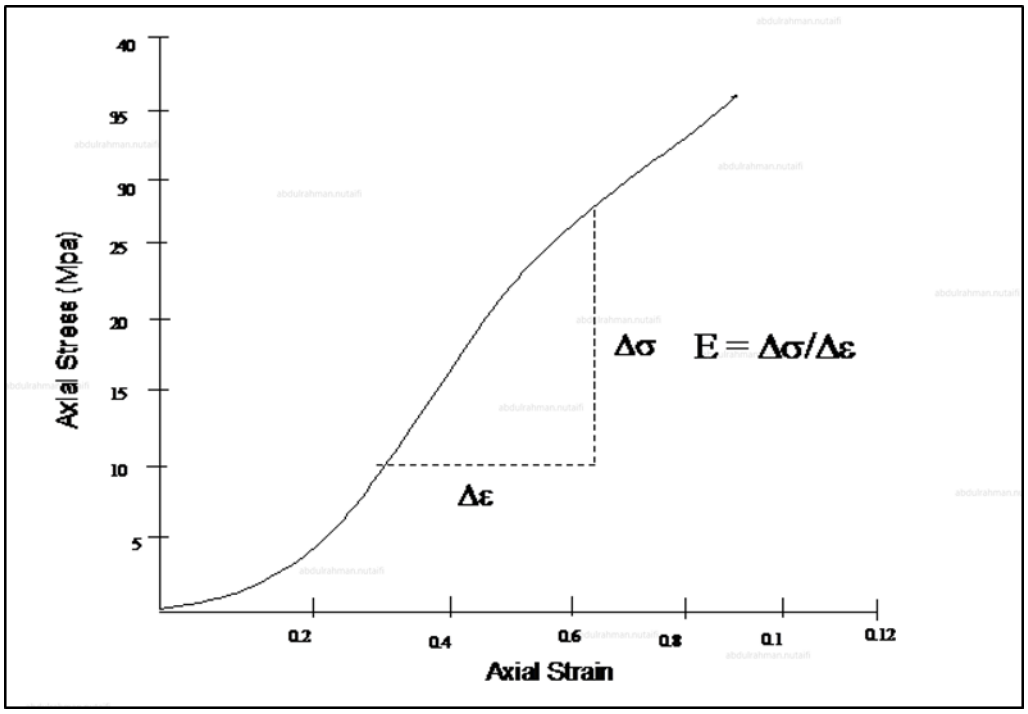

Figure 6: Stress strain relationship for a given confining pressure. Zoback [2007]

Poisson's ratio (ν) describe the relationship between the different directions of deformation "strain" of an object under stress "pressure" in both axial "direction of stress" and the radial "perpendicular to the stress direction. It is evaluated as the ratio of the axial contraction to radial expansion for the same linear section used to determine the Young's modulus as shown in equation 2.2. (Zoback ,2007).

$$v = \frac{Axial\ Strain}{Radial\ Strain} = \frac{\varepsilon_a}{\varepsilon_r} \qquad (2.2)$$

Where, ε_a is the axial strain and ε_r is the radial strain all measured in unit of length.

The dynamic elastic properties are measured by sending an ultrasonic acoustic signal through a rock sample and measuring its velocity. The acoustic signal will generate two types of waves; compressional (longitudinal) and shear (transverse) waves. Therefore, two velocities are measured from a standard dynamic testing; compressional velocity (Vp), and shear velocity (Vs).

The Biot coefficient (α) describes the level of compressibility the dry rock sample experience under applied stress compared to the rock matrix, Zoback [2007]. The Biot coefficient is defined as shown function of porosity as shown in equation 2.3.

$$\alpha = 1 - (1 - \phi)^{\frac{3}{1-\phi}} \qquad (2.3)$$

Where, $\emptyset$ is the estimated porosity, range between dry sample and fully saturated.

Unconfined Compressive Strength (UCS) is an important parameter to determination the rock failure condition. It is defined as the maximum axial compressive stress that material can withstand under unconfined conditions (zero confining pressure) before it fails "breaks". UCS is estimated using several confining pressures' peak strength data applying a rock failure criteria to be discussed in upcoming sections. (Zoback,2007).

2.4 Correlations of Dynamic Properties for 1D MEM

Overburden Stress

The overburden stress at a certain depth is defined as the weight of the rock column from the surface down to required depth. Equation 2.4 shows the overburdens stress as function of rock density, Zoback [2007].

$$\sigma_z = \int_0^z \rho(z) \cdot g \cdot dz \qquad (2.4)$$

Where, σ_z is the overburden stress at depth z,

ρ is formation bulk density,

g is gravitational acceleration constant.

The overburden stress need to be estimated to the surface (depth=0). The formation density is measured using open hole logs (RHOB) and in most of the cases only for the formation and not for all the overhead layers. A wide range of empirical relationships are available

for estimating the density magnitude using several data attributes are available in the literature. Gardner and Harris [1968] developed empirical correlations, which derives the density from sonic or seismic data as shown in equation 2.5.

$$\rho_{Gardner} = \alpha \times V^{\beta} \qquad (2.5)$$

Where, α and β are two fitting parameters named velocity factor and velocity exponent, V is the wave velocity derived from sonic logs or seismic data.

In the Gardner original equation, α and β are set to 0.23 and 0.25 respectively.

Traugott [1966] used porosity data as the base for extrapolating the density using log data across the logged interval. His method utilizes an iterative workflow. Amoco [1988] using data from the Gulf of Mexico, developed an extrapolation technique to estimate bulk density as shown in equation 2.6.

$$\rho_{Amoco} = \rho_{MudLine} + A_0 \times [\frac{(TVD - AirGap - WaterDepth)}{3125}]^{\alpha} \quad (2.6)$$

Where, $\rho_{MudLine}$ the density at mudline level

α is fitting exponent with a value of 0.6.

Miller [1995] developed a porosity based prediction correlation used in predicting density as shown in equations 2.7 and 2.8.

$$\rho_{Miller} = \rho_{Matrix} \times (1 - \phi_{Miller}) + \phi_{Miller} \times \rho_{Water} \quad (2.7)$$

$$\phi_{Miller} = \phi_a + \phi_b \times -[k(TVD - AirGap - WaterDepth)]^{\frac{1}{N}} \qquad (2.8)$$

Where, ρ_{Matrix} is the average matrix density,

ρ_{Water} is the water density. ϕ_a and ϕ_b are two reference porosity measurements with default value of 0.35. k is the porosity decline parameter and N is the curvature parameter (default values of 0.0035 and 1.09 respectively).

Wendt al, [2007] developed a method for estimating density from acoustic compressional slowness using data from Kvitebjorn field in the Norwegian North Sea an shown in equation 2.9. The compressional slowness data is derived from open hole log measurement.

$$\rho_{Wendt} = 3.967 - 0.00691 + DT + E^{-5}1.9(DT)^2 + E^{-8}4.7(DT)^3 + 0.05471\tan^{-1}\frac{(BHT - 234.6)}{26.75} \qquad (2.9)$$

Where, DT is the compressional slowness. BHT is the bottom-hole temperature.

Other methods of estimating density include assuming a constant density value across the whole interval, which might endure additional error. Also, density data can be fitted using equation 2.10.

$$\rho_{extrapolated} = \rho_O + A_0\,(TVD)^{\alpha} \qquad (2.10)$$

Where,ρ_O is the density at the surface. A_0 and α are the fitting parameters found to be around 0.013 and 0.36 respectively.

Young's modulus

Morales and Marcinew [1993] published correlations to estimate static Young's modulus from calculated dynamic data using core data of high-permeability sandstones ranging from very fine-grained to coarse-grained from several fields, including Kuparuk, Alaska; Elmworth and Mitsue, Canada; Punta Benitez and Boqueron, Venzuela. This is applicable to all three porosity groups: consolidated (10%-15%), moderately consolidated (15%-25%), and weakly consolidated (>25%). The below are the correlation for each respective porosity range;

$$\log(Es) = 2.137 + 0.6612 \times \log(Ed)$$, for (Porosity 10%-15%) (2.11)

$$\log(Es) = 1.829 + 0.6920 \times \log(Ed)$$, for (Porosity 15%-25%) (2.12)

$$\log(Es) = -0.475 + 0.9404 \times \log(Ed)$$, for (Porosity >25%) (2.13)

Where, E_s is the static Young's modulus and E_d is the dynamic young's modulus.

Bratton [1997] modified Morales correlation to include the total porosity based on the same dataset used in Morales paper. Fuller et.al [2000] studied sandstone dataset from the North Sea and developed a best fit exponential correlation which is shown in equation 2.14.

$$Es = 0.0018 \times Ed^{2.7} \qquad (2.14)$$

Poisson's Ratio

To calculate the Poisson's ratio, a multiplier method is used to convert from dynamic Poisson ratio. Krief [1990] developed a correlation that assumes that Biot coefficient can be estimated from the effective porosity as in equation 2.3 shown earlier.

Unconfined Compressive Strength (UCS)

Several correlations are available in the literature to estimate UCS from various parameters. Plump [2002] developed several models to estimate UCS from shear modulus, static Young's modulus and porosity. The first correlation was based on the rock dynamic shear modulus. It was originally reported by Gholkar and Plumb [1996], and updated by Plumb [2002]. The correlation is defined by laboratory measurements on sands and silty sands over the porosity range of 0%–40%. The second correlation was porosity-based correlation (clay, grain or upper bound porosity) which are useful when there is no sonic data available to calculate the shear modulus. Rzhevesky and Novak [1971] developed a correlation based on data from the Korobcheyev field, Russia relating UCS to porosity as follows,

$$UCS = 276 \times (1 - 3\phi)^2 \qquad (2.15)$$

Horsrud et.al [2001] developed a correlation to relate UCS to sonic data. The developed empirical correlation relation relates UCS to the compressional slowness DTCO using equation 2.16.

$$UCS = 0.77 \times (\frac{304.8}{DTCO})^{2.93} \qquad (2.16)$$

Friction Angle (FANG.)

Several correlations are available in the literature to estimate the Friction Angle from gamma ray log and porosity. Weingarten and Perkins [1988] developed a correlation between F.A. and porosity in sandstone data an shown in equation 2.17 and 2.18;

$$F.A. = 58 - 135\phi \qquad (2.17)$$

$$F.A. = 57.8 - 105\phi \qquad (2.18)$$

A cutoff method is applied to FANG. from available gamma ray logs. With default parameters, GR 120 gAPI is mapped to FANG 20 degree and GR 40 gAPI is mapped to FANG 35 degree. If the calculated FANG is less than 15 degree, it is forced to 15 degree. If it is greater than 40 degree, it is forced to 40 degree as shown in Figure 7.

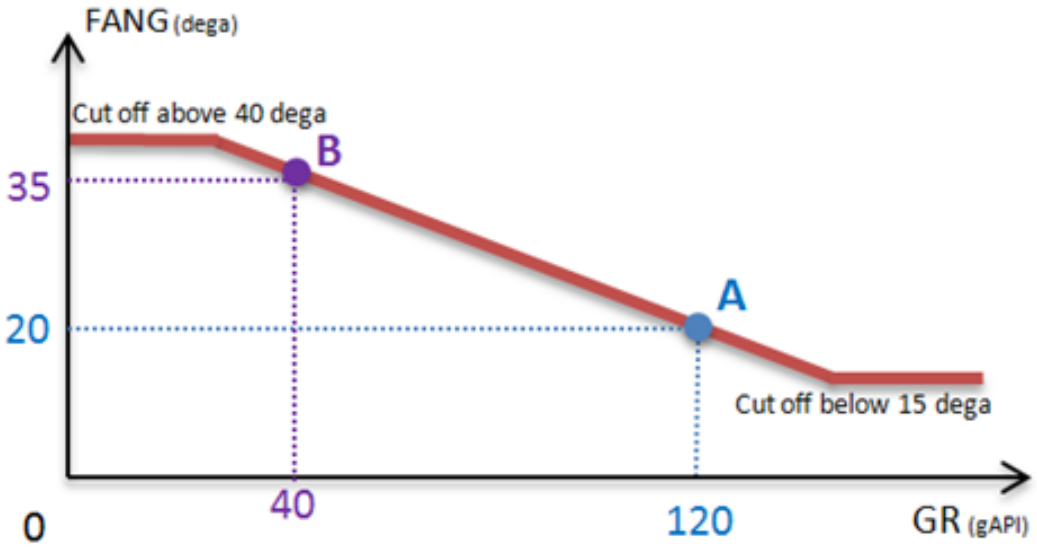

Figure 7: FANG Estimation using GR cutoff after Weingarten and Perkins [1988]

A number of powerful numerical geo-mechanical commercial simulations software exist which can be used for advanced borehole instability modeling. These models include finite difference codes, distinct element codes and finite element codes. These models are capable of representing a realistic rock deformation. In this study TECHLOG™ platform is utilized in the analysis and modeling work, which is developed by Schlumberger.

2.5 Natural Fracture Role in Wellbore Instability

In heavily faulted carbonate reservoirs, the presence of the natural fractures is observed. They form due to the variation in earth stress tensors and tectonic plates' movement (Zoback, 1989). Natural fractures can be classified depending on whether they are, conductive (open) or resistive (healed) fractures. In Open fractures, the area between the fracture surfaces is empty and provide a conduit for flow by creating a high perm streak that can reach up to several Darcy's an opposed to normal permeability ranges in a matrix of few hundred mDarcy's (Lorenz,1990). However, if the area is filled with a cementing material, usually calcite which is not permeable, and then the fracture conductivity drops. The type of layers fractures exists in and their mechanical property and strength will determine the extension and geometry of the fractures (Nelson, 1985). On the other hand, induced fractures can be created using excessive mud weight one the hydrostatic pressure exceed the safe mud weight window and even the fracturing gradient which might create complete loss of circulation. Santarelli. [1992] showed field cases of drilling through fractured shale reservoir where optimizing the drilling fluid has great impact on the smoothness of drilling operation. Mclellan [1996] proposed that fluid density alone is not enough to reduce the risk of loss circulation while drilling in a fractured environment. This was further confirmed with work from Edwards et.al [2002] where he deduced that excessive mud weights while drilling weakened planes such as fractures by destabilizing the wellbore even further. Nquyen and Abousleiman [2009] showed that fractures could have considerable width in shale reservoirs. There are few reported case studies on fractured environment in carbonate reservoirs. Approaches to model such environment is

by creating dual-porosity dual permeability poro-elastic models where the matrix properties and fractures properties are reported in the literature.

In reservoir studies, natural fracture contribution to the reservoir porosity and permeability is studied. Nelson (1985) provided a classification of the naturally fractured reservoirs based on natural fracture contribution to reservoir properties as shown in Figure 8.

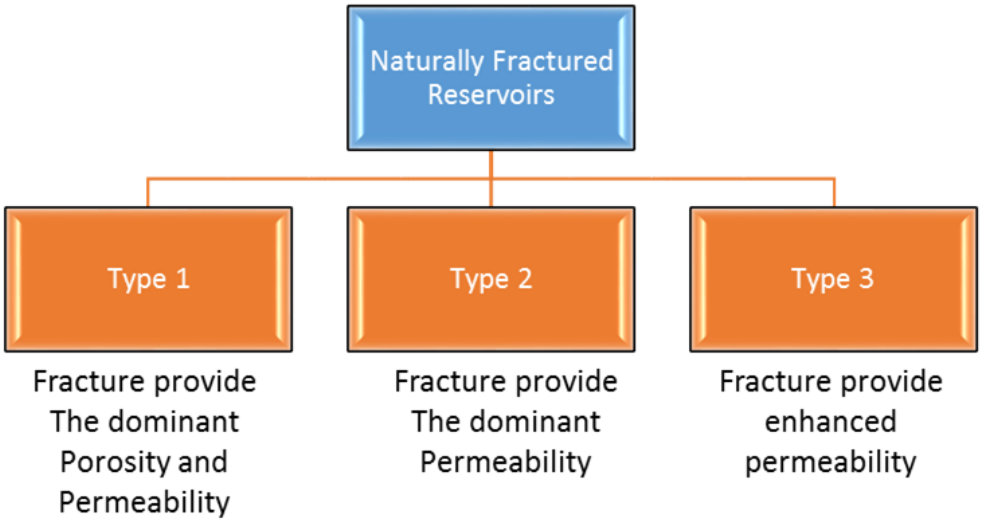

Figure 8: Naturally fractured reservoirs classification (Nelson, 2001)

On the other hand, and as previously discussed, excessive mud weight used in drilling operations would create induced fractures if the fracture gradient pressure is exceeded. Those fractures are usually smaller than natural fractures and their size and propagation depend on the stress state of the reservoir rock. Some recent work from Sirat [2015] and Mehrabian [2015] showed utilization of 1D MEM model can help in predicting the loss circulation events through construction of the Safe Mud weight windows. However new

development in borehole imaging had enabled researches to further develop better in understanding of the natural fractures characterization.

The development of image technologies had helped in description the existence and classification post drilling operations (Zemanek, 1969). Two main measurement bases are used in image logging, resistivity based or acoustic “ultrasonic”. In principle, image log tools acquire a full borehole data opposed to the single directional conventional logging tools (Kulander, 1990). This provide additional features on the continuity of features such as fractures. The tool is additionally occupied with several orientation caliper arms that can measure the engagement of the hole and orient the measured data. In this study, an image log interpretation will be used to describe the type of fractures using a commercial software provided from other studies. Natural fractures are usually sinusoidal in shape and fully covering the borehole and not in consistent with the bedding planes. (Timur ,1987)

2.6 Natural Fractures Modeling from Static and Dynamic Data

Zhang [2017] developed an integrated workflow for modeling various scales of natural fracture to create a Discrete Fractures Network model (DFN). His model integrates, outcrop data, core data, image log analysis, seismic data analysis, drilling data analysis, well testing data analysis, production data analysis as well as lab analysis of fractured conceptual model to build a holistic understanding of the fractures parameters and density across the studied area. He also examined the effect of various elements such as faults, structure deformation, rock mechanics and earth stresses on natural fractures distribution. Kuchuk [2014] discussed the limitation of the dual porosity dual permeability modeling

widely used to describe natural fractures in the industry. He proposed a fractured reservoir model that is capable of treating thousands of fractures that are periodically or arbitrarily distributed with finite or infinite conductivities, different lengths, densities, and orientations. He showed variation between the fracture and matrix permeability can impact the validity of the dual porosity dual permeability modeling. His work focused on the modeling of pressure transient behavior and provided well scale insight on the complexity of natural fracture modeling. Fonta [2005] utilized both stochastic techniques and seismic attributed based modeling for both small and large scale natural fractures modeling in The Najmah reservoir of west Kuwait. He highlighted the use of the seismic facies analysis (SFA) and specific seismic data attribute selection in developing the basis for the discrete natural fracture modeling. Ozkaya [2016] demonstrated how the location, size, and shape of interconnected-conductive-fracture bundles can be determined by integrating borehole-image data with depletion- curve analysis. Al-Omair [2010] illustrated various methods to detect natural fractures from different static and dynamic data sources. In his work, an integrated workflow from fractures detection, mapping and validation was developed for modeling natural fracture in Saudi Aramco event solution projects. For fractures modeling, factures properties population were integrated with the simulation models and history matched with dynamic data (production, injection and pressure data) to reduce the risk associated with the model. Ateeq [2018] illustrated an integrated workflow to account for accumulated knowledge of natural fractures properties data distribution from various data attributes into the dynamic simulation for a carbonate gas condensate field in Abu Dhabi. The fracture networks occurring in the reservoirs were characterized using core, borehole-image, 3D-seismic, and dynamic data. Fracture-characterization results from seismic and

well data were integrated into a conceptual fracture model which was up scaled and calibrated dynamically using the well-test production data.

CHAPTER 3

DATA DESCRIPTION AND PROBLEM QUANTIFICATION

The reservoir under study is a carbonate reservoir where the reservoir quality is prolific. It is classified as high relief, four-way dip closure structure, and paleogeographic facies consisting of carbonate shoals and tidal inletsret. Analogues fields shows that the targeted reservoir is known to be variable due to localized and often extensive diagenetic overprint. The formation is deposited in the late Permian and mainly classified into three main reservoirs A, B and C separated by layers of anhydrite.

3.1 Data Description and Data Quality Check

Table 1 shows the available data that was used in the analysis:

- Available well logs, drilling reports and open hole logs for the wells drilled in the field to the study date.
- Rock mechanical properties obtained from lab testing.
- Available well test, pressure measurement and formation testing data.
- Image log data with fracture interpretation.

Table 1: Available wells data included in the study

Well	Drilling Daily Reports	Loss Circulation Data	Open Hole Logs	Core Data	Core Plug Mech. Properties	Pressure Data	Image Logs	Pressure Transient Data
Well-A	✓	✓	✓	✓	✓	✓	✓	✓
Well-B	✗	✓	✓	✓	✓	✓	✓	✓
Well-C	✗	✓	✓	✓	✓	✓	✗	✓
Well-D	✓	✓	✗	✗	✗	✗	✗	✗
Well-E	✓	✓	✗	✗	✗	✗	✗	✗
Well-F	✓	✓	✓	✓	✗	✗	✓	✗

3.2 Quality Check for Available Data

The quality of the collected logs was continuous and noise free, however it was affected in some parts by the severity of the loss circulation events resulting in sizeable invasion zones, yet the quality is considered good enough to be utilized for further analysis. Available core data was fully described. Elastic properties and rock strength measurements were available from several plugs carried out in the lab. Six wells were included in this study; Well-A, B, C, D, E, and F represents a wide geographical area and has a good coverage of the field. Available drilling reports were reviewed and loss circulation events were summarized in order to be utilized.

3.3 Reservoir Properties Description

Core data from Well-A and Well-B were used to investigate the reservoir properties changes within the reservoir layers. Figure 9 and 10 shows histograms of porosity measurement form two wells. Porosity from both wells shows multi-mode distribution

which is a clear indication of heterogeneity in the reservoir. The impact of heterogeneity on the analysis of the wellbore instability will be discussed in upcoming sections.

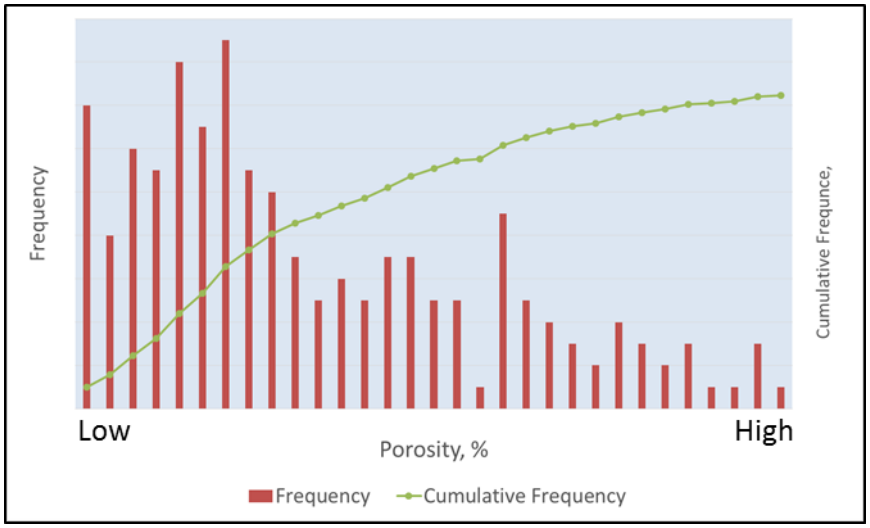

Figure 9: Well-A core porosity measurement histogram showing clear identification of heterogeneity

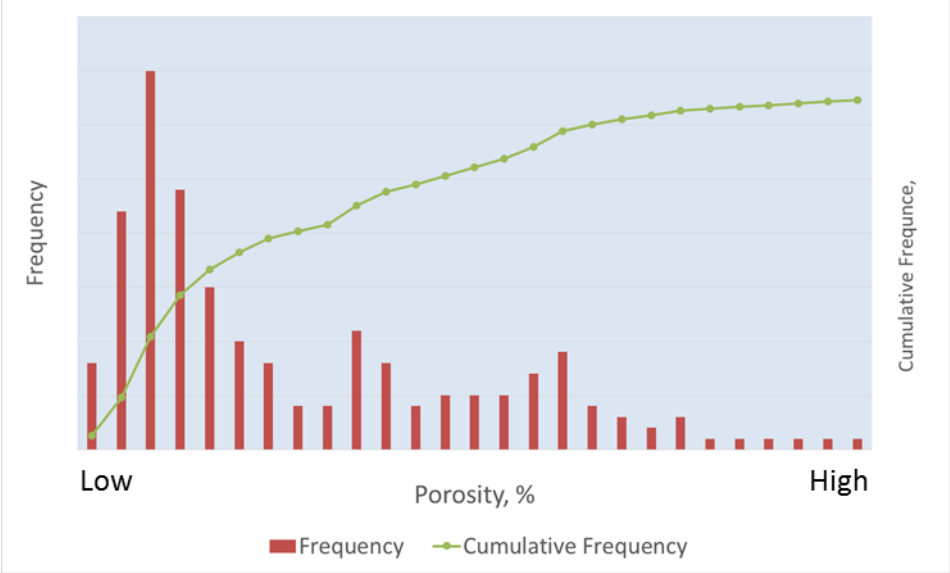

Figure 10: Well-B core porosity measurement histogram showing clear identification of heterogeneity

3.4 Wells Datasets Selection

After reviewing the available data, Well-A and Well-F were used to build the 1-D MEM. This was due to having the full needed set of loss circulation data, rock mechanical properties and Image logs available in these wells. The rest of the wells data will be used in calibrating the MEM models for Well-A and Well-F, analyzing the loss circulation events and build a predictive model for loss circulation events future drilling programs.

3.5 Laboratory Testing for Rock Mechanical Data

Well-A and Well-F wells were cored across the reservoir section. Selected core plugs were used to estimate the rock mechanical properties using the New England Research (NER) Multi-Stage Tri-axial testing equipment shown in Figure 11 conducted in Saudi Aramco.

Figure 11: New England Research Multi-Stage Tri-axial testing equipment

Sample Preparation

Sample Preparation includes the following steps:

- Core plug selection from a given interval.
- Surface grounding of the parallel end faces until they become flat to within 0.001 inches.
- Jacketing of the plug and positioning of two end caps equipped with velocity transducers on the ends of the sample while a coupling medium is set between the plug flat surfaces and the transducer.

Sample Loading

Figure 12 shows the chamber where the core plugs were loaded. After completing the sample preparation as per the procedure above, the plug will be equipped and loaded onto the testing frame as follows:

- The jacket is clamped to the transducers from both ends to allow for hydraulically applying confining pressure around the sample.
- Radial and axial LVTDs are positioned around and along the sample to measure radial and axial displacements respectively.
- Confining pressure is applied hydrostatically around the sample. The confining pressures are selected to simulate the stress condition in the vicinity of the wellbore.

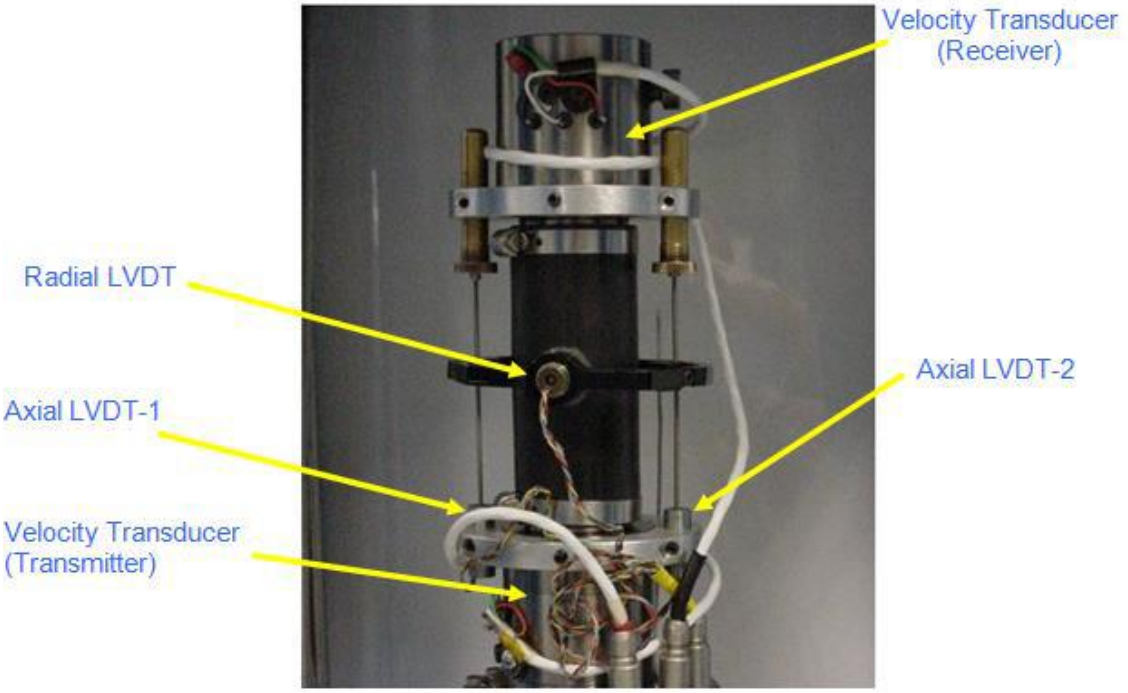

Figure 12: Core Plug Chamber

Sample Testing

Multi-stage triaxial loading are performed on selective samples which involve loading the rock sample at a given confining pressure to failure (single stage) or near failure (multistage) then a new sample is tested or a new loading cycle is applied on same sample using a different confining pressure. A Mohr-Coulomb failure envelope is then constructed from three to four tested samples or three to four loading cycles.

For multistage loading a sample is hydrostatically loaded to a given confining pressure and the differential axial stress is increased slowly until a non-linear radial strain is observed

upon which the sample is unloaded and a new confining pressure is applied to go through the next loading stage. Multi-stage loading is applied when it is determined that the sample is a good candidate for such testing methodology. It must be emphasized that the sample must not be loaded beyond the initiation of a plastic deformation.

The dynamic elastic properties are determined simultaneously with the static properties using ultrasonic measurements. The static properties are required for many petroleum engineering applications; however, dynamic data are often collected in the field and therefore necessary calibration must be obtained to design certain treatments such as wellbore stability, hydraulic fracturing, and sand control.

To perform dynamic measurements (ultrasonic velocity measurements) the end caps of the core sample are equipped with ultrasonic transducers and receivers which can generate and detect both compressional and shear waves. One transducer is a transmitter which induce an ultrasonic wave at a frequency of 700 kHz and the other one is a receiver. In this work the velocities of these waves are used to compute the dynamic Young's modulus and Poisson's ratio.

Data Collection

Figure 13 shows the data collection console. During the test, the following data are collected:

- Vertical stress which is applied axially at an axial displacement rate of 3-6 mm/hr (4-8% strain). The loading rate is applied such that failure or near failure is reached within 5-15 minutes.

- Axial strain is measured from the two LVDTs positioned on two locations along the axis of the sample. The axial strain is calculated from averaging the readings of the two LVDTs.
- Radial strain from the radial LVDT.
- Confining pressure as provided by the confining fluid.
- Velocity measurements are performed by sending ultrasonic signal axially and the compressional and shear velocities are measured via the velocity transducers.

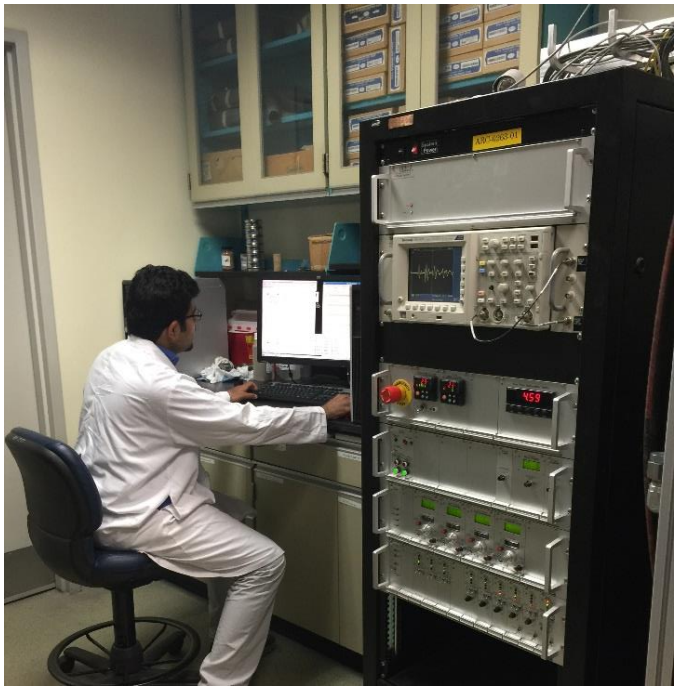

Figure 13: New England Research Multi-Stage Tri-axial testing equipment Data Collection Counsel

In this study, a Uniaxial Compressive Strength (UCS), Friction Angle and Cohesion are calculated graphically for all the plugs subjected to multistage testing through a Mohr-Coulomb failure envelope. Table 2 shows a summary of the mechanical properties of the core plugs of Well-A and Well-F included in the evaluation.

Table 2: Summary of the mechanical properties of the core plugs of Well-A and Well-F included in the evaluation

Sample #	Depth	Bulk Density	Confining Pressure	Young's Modulus		Poisson Ratio		Peak Strength	UCS	FANG	Cohesion	Shear Angle
		(Dry)		Static	Dynamic	Static	Dynamic					Calculated
	(ft.)	(gm/cc)	(PSI)	(MPSI)	(MPSI)	(Ratio)	(Ratio)	(PSI)	(PSI)	(Degree)	(PSI)	(degree)
1	12,142.2	2.5	741.5	4.7	7.7	0.2	0.2	17,254.6	12,360.2	47.2	2,423.4	68.6
2	12,172.2	2.5	741.5	4.9	8.1	0.3	0.3	14,500.5	11,409.5	38.9	2,728.1	64.4
3	12,201.2	2.7	741.5	3.9	9.5	0.3	0.3	13,394.4	11,278.4	29.7	3,277.9	59.8
4	12,204.2	2.2	736.6	4.8	5.5	0.3	0.3	12,536.9	10,165.6	35.1	2,642.1	62.5
5	12,271.8	2.8	746.4	6.3	10.8	0.4	0.3	16,042.1	11,417.7	46.9	2,255.0	68.4
6	12,328.6	2.9	746.4	6.3	10.8	0.4	0.3	16,042.1	18,215.1	39.2	4,326.3	64.6
7	12,335.1	2.9	736.6	10.1	12.6	0.3	0.3	17,479.5	14,226.6	38.3	3,449.4	64.1
8	12,338.7	2.9	746.4	11.2	13.2	0.2	0.3	21,603.3	17,339.8	44.7	3,621.8	67.3
9	12,345.5	2.9	746.4	9.8	12.4	0.3	0.3	19,995.3	15,680.5	45.0	3,249.4	67.5
10	12,354.5	2.9	741.5	11.4	12.2	0.3	0.3	21,454.9	17,969.5	43.0	3,907.9	66.5
11	10,917.0	2.80	724.4	11.5	17.4	0.182	0.268	24,348.70	18,419.1	51.4	3,225.6	70.7
12	10,917.1	2.80	1,456.8	7.3	16.7	0.118	0.257	30,294.40				
13	10,917.8	2.66	2,201.3	3.9	11.4	0.224	0.330	20,122.4				
14	10,938.2	2.64	734.1	6.8	11.3	0.184	0.227	19,279.4	13,442.6	54.5	2,150.1	72.8
15	10,938.4	2.69	1,462.8	8.8	14.1	0.258	0.248	30,428.2				
16	10,938.7	2.62	2,181.9	7.7	12.1	0.239	0.259	34,086.3				
17	10,950.7	2.46	1,472.1	7.1	11.9	0.265	0.266	21,862.3				
18	10,965.0	2.10	737.6	2.4	3.8	0.256	0.294	7,540.8	5,374.1	29.5	1,567.8	59.7
19	10,965.6	2.05	2179.3	2.5	4.2	0.165	0.259	11,775.6				
20	10,965.2	2.19	1,481.5	3.2	4.8	0.195	0.295	13,171.1				

3.6 Definition of Wellbore Instability Problem

Sever wellbore instabilities during the drilling operations for the field under study was experienced since the first drilling operations. In order to understand the problem of wellbore instability, all relevant drilling, geological and log data for the problematic wells need to be considered and analyzed. Having a wide range of data for these wells we will be able to conduct a post-mortem analysis referred to in this study as Drilled Wells Analysis which will help elucidate and pin-point the main factors causing borehole instability. In this study, loss circulation events will be the primarily focus since it is the dominant wellbore instability problem encountered in the field under study.

Before setting out to analyze the well data for identifying instances for instability, it is prudent to propose a working definition of borehole instability pertinent to the field under study. Based on consensus published in the literature, a section of uncased borehole is considered instable when sever mud loss circulation is experienced during drilling operations.

The field under study is an offshore field developed by drilling vertical and highly deviated wells in naturally fracture reservoir deduced from core and well test data. Deviated wells were directed as all drilling operations were conducted from platforms. Experience form drilling over twenty drilled wells showed highly problematic wellbore instability issues are mainly sever loss circulations. This has resulted in huge lost drilling time and in some cases total well loss. Knowledge of rock mechanical properties in wellbore the stress state in the field as well as the safe mud weight windows is required to meet all challenges associated with future wells drilling program.

3.7 Problem Quantification

A statistical approach was used to quantify the loss circulation experienced while drilling the reservoir in field under study. Data for this analysis was obtained from the daily drilling morning reports for the twelve wells that was considered in this study. Tables 3-6 shows the mud losses across reservoir section, mud weights used while drilling across reservoir, time curing these losses and time spent to drill the reservoir to total-depth. 32 loss circulation events were logged in the analyzed wells as shown in Tables 3-6. The events log includes the type of operation either drilling in the reservoir section or mitigating circulation while curing the loss circulation, loss circulation volume and average loss circulation rate.

Table 3: Well-A Daily Loss Circulation Volume and Rate Consolidated from Daily Drilling Report (DDR)

Date	Month	Day	Year	Depth, MD	Operation	Loss Volume , BBLs	Lost Cri. Rate BBL/hr
Mon	Jan	23	2006	11010	Drilling	102	4
Fri	Feb	3	2006	11302	Drilling	300	13
Sat	Feb	4	2006	11302	Maintaing Cir.	1500	63
Thu	Feb	16	2006	11724	Drilling	375	16
Fri	Feb	17	2006	11990	Drilling	50	2
Mon	Jun	5	2006	14016	Maintaing Cir.	667	28
Sat	Jul	8	2006	12775	Maintaing Cir.	50	2

Table 4: Well-D Daily Loss Circulation Volume and Rate Consolidated from Daily Drilling Report (DDR)

Date	Month	Day	Year	Depth, MD	Operation	Loss Volume , BBLs	Lost Cri. Rate BBL/hr
Mon	Dec	14	2009	10745	Drilling	1159.5	48
Tue	Dec	15	2009	10756	Drilling	120	5
Wed	Dec	16	2009	10817	Drilling	600	25
Thu	Dec	17	2009	10817	Maitaining Cir.	320	13
Sat	Dec	19	2009	10907	Drilling	250	10
Tue	Dec	22	2009	11127	Drilling	300	13
Sun	Dec	27	2009	11725	Drilling	610	25
Mon	Dec	28	2009	11751	Drilling	260	11
Thu	Jan	7	2010	11897	Maitaining Cir.	10	0

Table 5: Well-E Daily Loss Circulation Volume and Rate Consolidated from Daily Drilling Report (DDR)

Date	Month	Day	Year	Depth, MD	Operation	Loss Volume , BBLs	Lost Cri. Rate BBL/hr
Fri	May	15	2009	12527	Maitianing Cir.	658.5	27
Sat	May	23	2009	13103	Drilling	906.5	38

Table 6: Well-F Daily Loss Circulation Volume and Rate Consolidated from Daily Drilling Report (DDR)

Date	Month	Day	Year	Depth, MD	Operation	Loss Volume , BBLs	Lost Cri. Rate BBL/hr
Fri	Mar	1	2013	11490	Drilling	875	36.5
Sat	Mar	2	2013	11490	Maitianing Cir.	3000	125.0
Sun	Mar	3	2013	11490	Maitianing Cir.	1250	52.1
Mon	Mar	4	2013	11490	Maitianing Cir.	2200	91.7
Tue	Mar	5	2013	11490	Maitianing Cir.	1720	71.7
Wed	Mar	6	2013	11490	Maitianing Cir.	1350	56.3
Thu	Mar	7	2013	11490	Maitianing Cir.	1450	60.4
Fri	Mar	8	2013	11490	Maitianing Cir.	960	40.0
Sat	Mar	9	2013	11490	Maitianing Cir.	1100	45.8
Thu	Mar	14	2013	11533	Drilling	520	21.7
Sat	Mar	16	2013	11591	Drilling	635	26.5
Sun	Mar	17	2013	11591	Maitianing Cir.	2200	91.7
Mon	Mar	18	2013	11591	Maitianing Cir.	863	36.0
Wed	Mar	27	2013	11968	Drilling	564	23.5

CHAPTER 4

OVERBURDEN STRESS AND PORE PRESSURE MODELS

Key components of any geomechanical model is the effective stress defined by the overburden stress and the pore pressure. Logging data from the six wells included in this study was utilized. Offset wells data are used. I also incorporated formation pressure (*i.e.* MDT and DST tests) while there are no available FIT tests' data.

4.1 Overburden Stress

Gravitational stress at any point in the earth is caused by the weight of the rock column overlaying that point. The overburden stress (σ_v) at depth, z, is calculated by integrating the weight above the point z using the following equation.

$$\sigma_v = \int z \, \rho \, dzg \quad (4.1)$$

Where, σ_v is the vertical/overburden stress (Pa), ρ is the formation bulk density (Kg/m^3)

g is the gravitational acceleration (m/s^2) z is depth (m).

Normally, overburden stress is vertical, so it is often called vertical stress. This stress value can be derived from average density of the overlaying sediments. Bulk density which is derived from available logs (RHOB) for the reservoir section can be used to calculate the

corresponding stress across those layers. However, a correction need to be made to fill in the gap where direct measurements are not available.

4.2 Methods for Estimating the Overburden Stress

In the literature review section, I summarized several available correlations and methods to estimate the density from available log data. well-A and well-B was used to validate the accuracy of these data. In this research, several statistical parameters were used to examine, diagnose, and visualize the prediction accuracy referenced to the actual bulk density measurement from logs. Four statistical parameters are applied as follows: Average absolute percent relative error AARE, maximum absolute percent relative error EMAX and relative error standard deviation ESt.D. Table 7 shows the summary of the results.

Table 7: Results of Bulk Density Extrapolation Method

Method Name	AARE	EMAX	ESt.D
Amoco	6%	114%	6%
Constant Density	13%	88%	6%
Extrapolation	15%	144%	11%
Miller	20%	70%	7%
Traugott	15%	79%	6%
Wendt	15%	78%	6%

As shown in Table 7, Amoco method showed the least average error percentage of 6% but error reached up to a maximum value of 114%. Therefore, I attempted developing a new

extrapolation correlation but utilizing all available sonic data from well data included in this study.

Global Extrapolation Method for calculating the Overburden Stress

Utilizing the density data for all wells included in this study, a generalized form of the extrapolation method was fitted the below equation as previously shown in the literature review section.

$$\rho_{extrapolated} = \rho_O + A_0 (TVD)^{\alpha} \quad (4.2)$$

Thus, all wells density data across the reservoir section was plotted. A best fit exponential curve in the form of equation 4.2 was fitted across the data as shown in Figure 14. The best fit, equation 4.3, is used to calculate the density of overlaying sections above the reservoir section where available logs are used.

$$\rho_{extrapolated} = 2.5 + 0.013 \times (TVD)^{0.36} \quad (4.3)$$

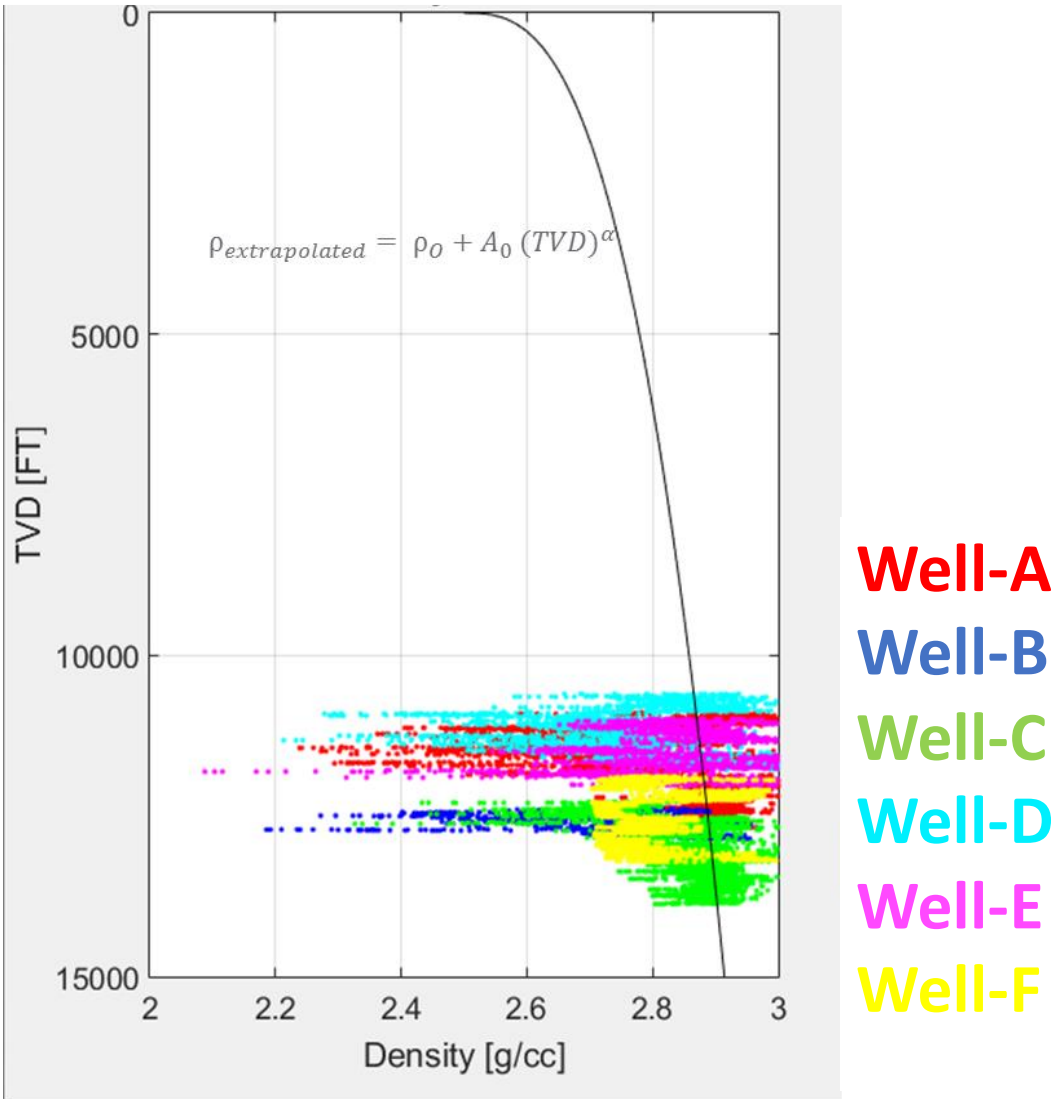

Figure 14: Matching the Log Bulk Density Data using Extrapolation Method

Table 8 shows the summary of the global bulk density extrapolation methods. The average error calculated was 5.1 % which is within acceptable range while the maximum error is around 30% compared to 114% using the Amoco method described earlier. As the

extrapolation method provided good match to the actual bulk density measurements from logs, equation (4.3) will be used to extrapolate the bulk density above the formation.

Table 8: Results of global bulk density using extrapolation method

Well Name	AARE	EMAX	ESt.D
Well-A	4.2	28.5	4.9
Well-B	6.8	32.3	6.25
Well-C	4.4	37.5	6.9
Well-D	5.7	38.1	5.4
Well-E	5.2	38.0	5.8
Well-F	4.1	6.8	1.8
Average	5.1	30.0	5.2

Figure 15 shows the calculated vertical stress (psi) and overburden MW (ppg) using the best fit curve from surface to TD. In the overburden stress above the reservoir section is estimated using the developed global extrapolation method. However, actual density data is used across logged reservoir section to improve accuracy.

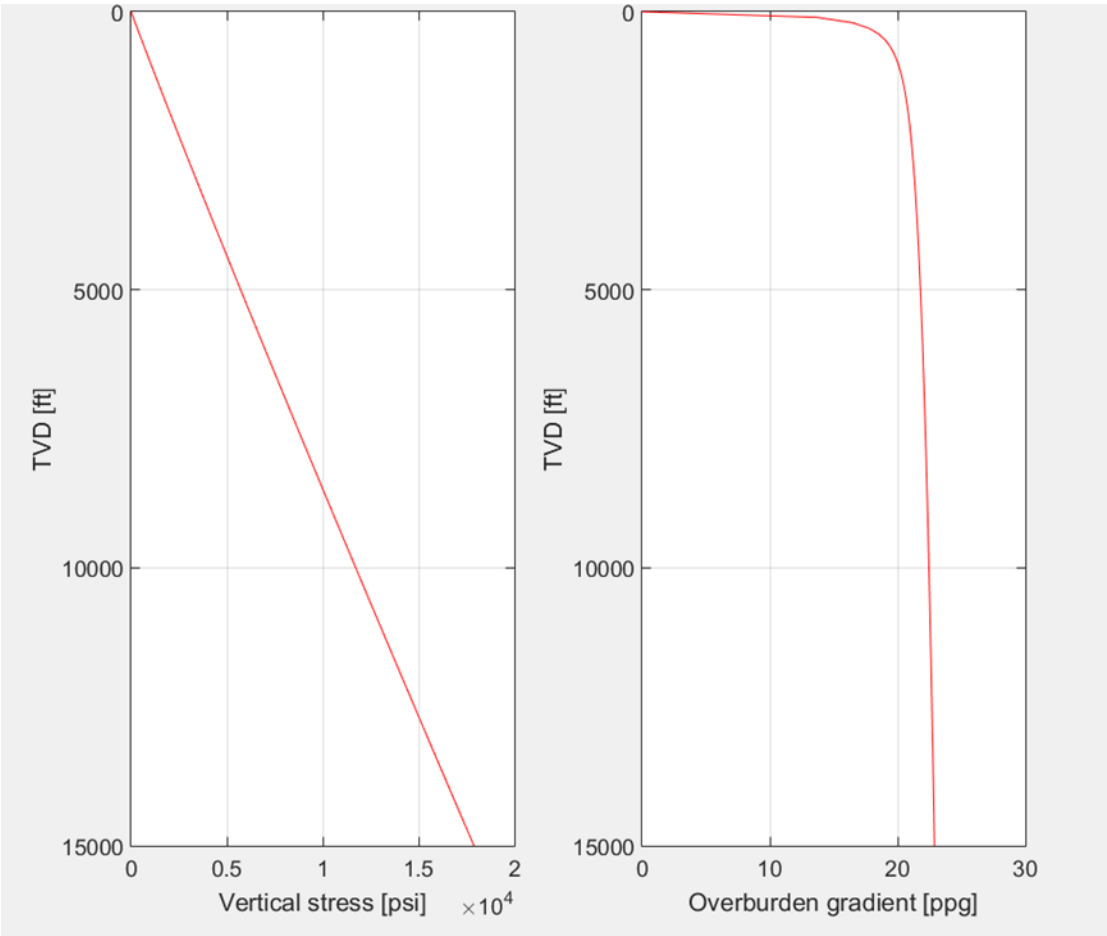

Figure 15: Calculated vertical stress (psi) and overburden MW (ppg) using the best fit curve from surface to TD.

4.3 Pore Pressure

Pore pressure plays a fundamental role in managing wellbore stability during drilling and production, defining stress magnitudes, and fracture gradient. As the pore pressure changes with time during the life cycle of a field due to production and injection processes, the stress magnitudes and fracture gradient changes accordingly. These stress changes can

influence the stability of wellbores as well as compaction and subsidence on the field scale in some cases. The overall effect of pore pressure changes is also influenced by the rock behavior including pore and bulk compressibility often referred to as the stress path of the field. All of the wells were drilled prior to the field production. Thus a single pore pressure model can be used as a good representation of pore pressure in the entire field. In three wells, A, B and C Modular Dynamic Tester data was collected which provided bases for establishing a hydrostatic gradient fit curve shown in Figure 16 for the pore pressure which will be utilized in the calculation in further chapters.

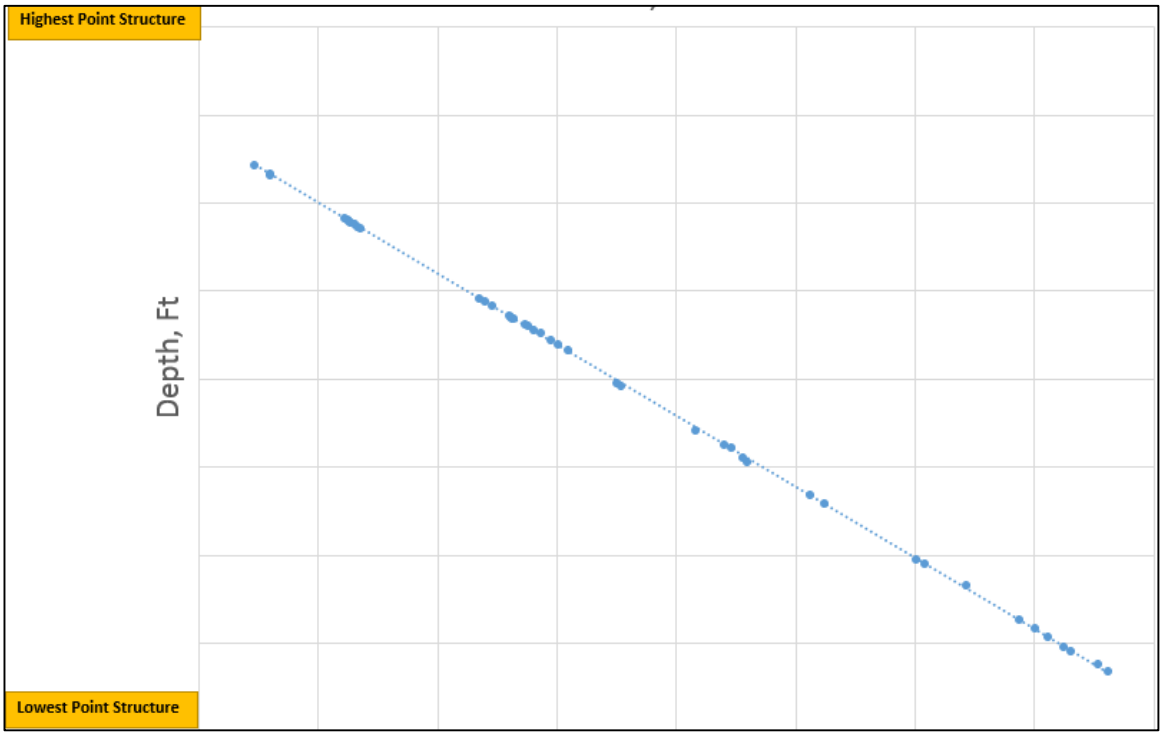

Figure 16: Wells A, B and C Modular Dynamic Tester data showing clear gas gradient (0.09psi/ft.) across the field

4.4 Rock Mechanical Properties

The mechanical response of rocks to changes in stresses is controlled by the mechanical properties of the rock. Understanding mechanical rock properties such as compressive strength, friction coefficients, Poisson's ratio and Biot's coefficient are an integral part of the geomechanical model. Therefore, an adequate laboratory testing program on core retrieved from the reservoir or formation of interest are valuable for providing accurate constraints for the required parameters.

Sonic tool is the only tool that respond to the elastic properties of the formation. When a pressure pulse is created in a wellbore filled with fluid, the complex phenomena that occur at the boundary between the wellbore and the formation results in the propagation of several types of waves into the formation. In this study a laboratory testing program was carried out. Single stage triaxial compression tests were conducted on core plugs from samples of two wells (Well-A and Well-F). Triaxial tests were conducted an dry core Twenty core plugs (20) triaxle compression tests carried out on dry plugs.

Given the assumption of a homogeneous, isotropic, and linearly elastic formation, dynamic shear and bulk modulus, G and K, can be computed from log measurement as follows:

$$G_{dyn} = (1347.45)\frac{\rho}{\Delta t\ Shear^2} \qquad (4.4)$$

$$K_{dyn} = \{(1347.45)\frac{1}{\Delta t\ comp^2})\} - \frac{4}{3}\ G \qquad (4.5)$$

Where, ρ is bulk density of the formation (g/cm3) which is a log measurement.

Δt_{comp} is compressional slowness of the bulk formation us/ft.

Δt_{Shear} is shear slowness of the bulk formation us/ft.

Dynamic Young's Modulus E and Poisson ratio (v) can be computed as follows:

$$E_{dyn} = \frac{9\, G_{dyn} \times 2KG_{dyn}}{3K_{dyn} + G_{dyn}} \quad (4.6)$$

$$v_{dyn} = \frac{3\, K_{dyn} - 2KG_{dyn}}{6K_{dyn} + 2G_{dyn}} \quad (4.7)$$

Figure 17 and Figure 18 shows the computed dynamic data for Well-A and Well-F respectively where YME_DYN track is the dynamic Young's modulus and PR_DYN track is the dynamic Poisson's ratio.

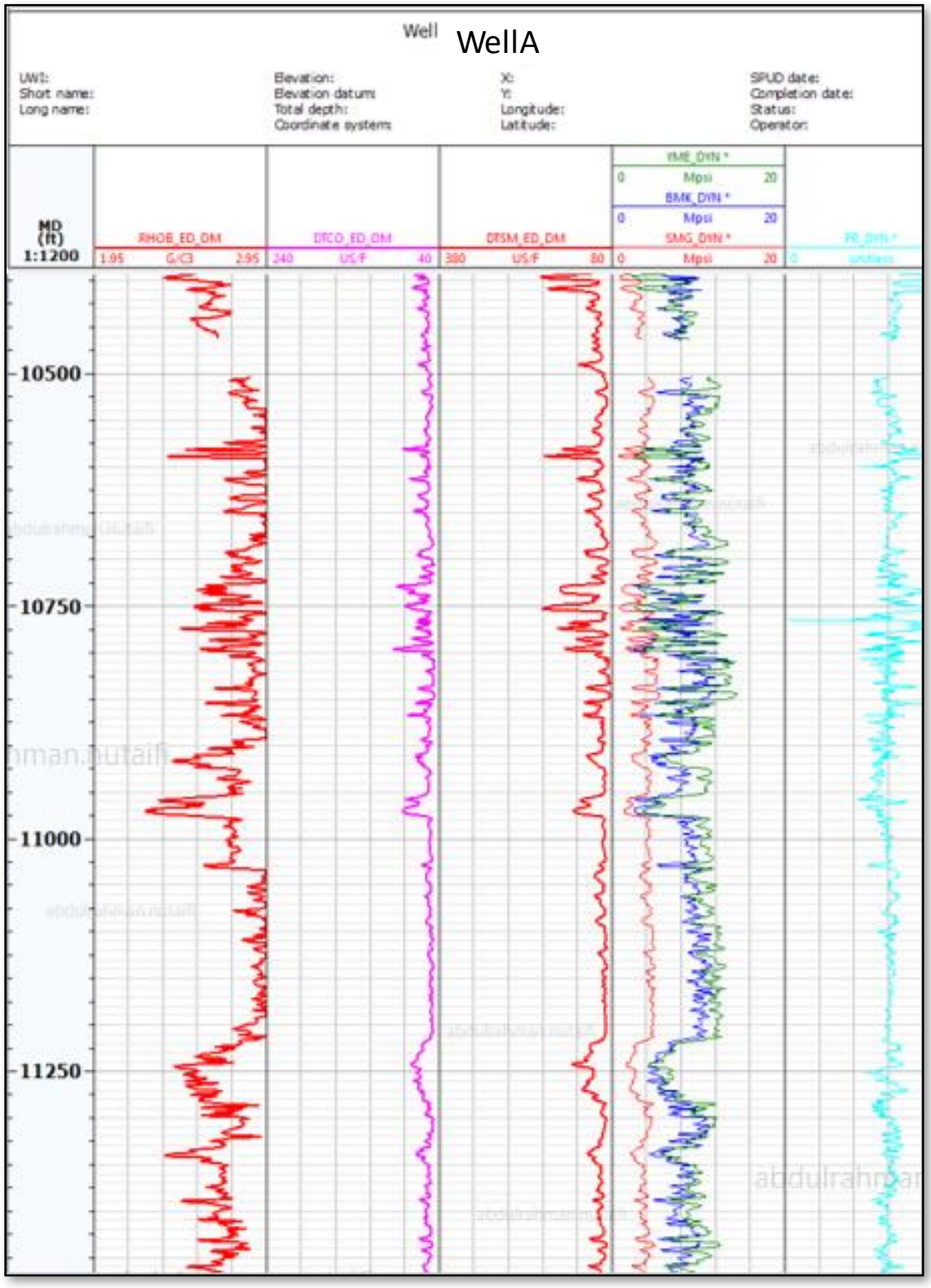

Figure 17: Well-A Dynamic Elastic Properties

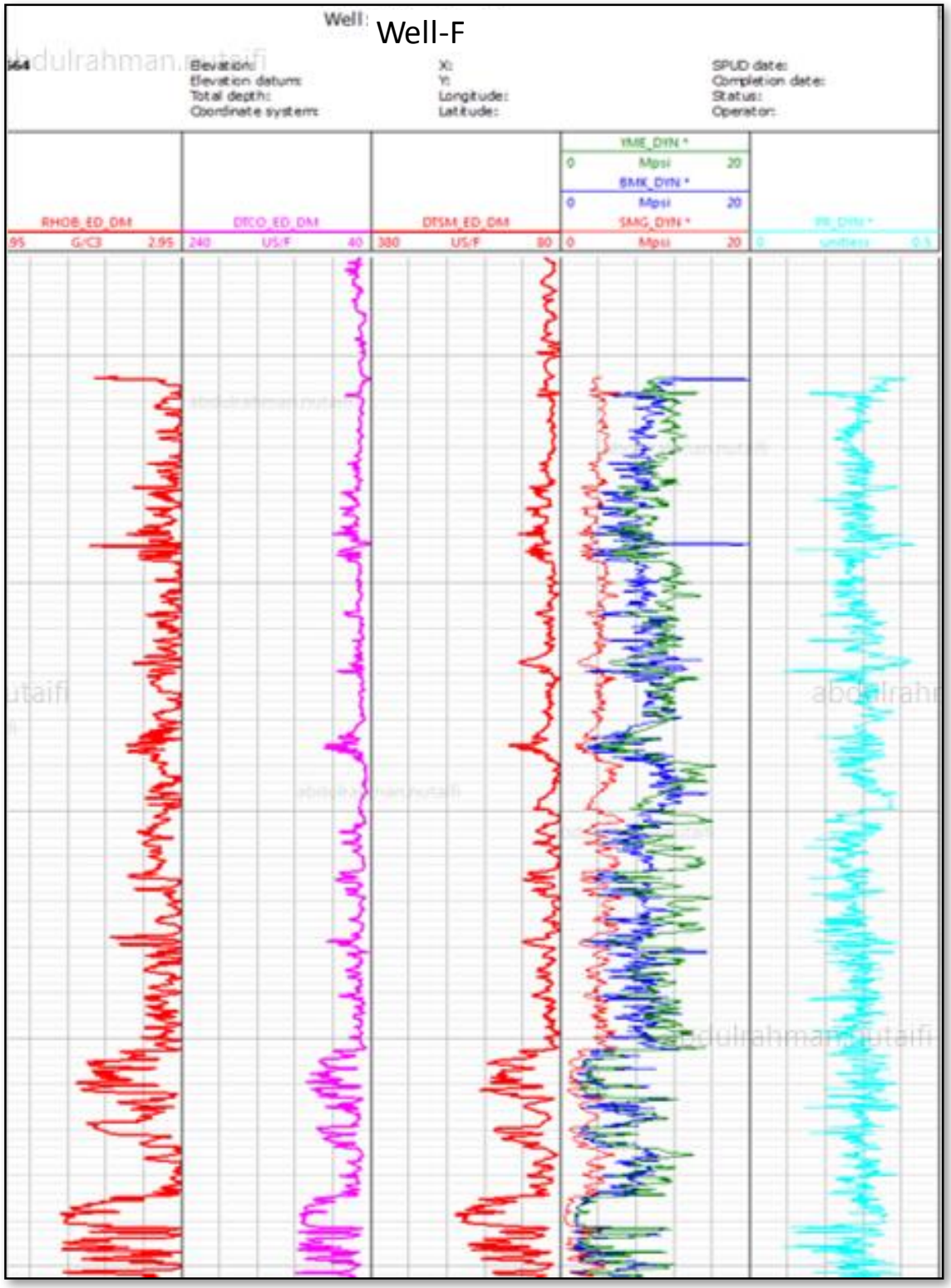

Figure 18: Well-F Dynamic Elastic Properties

4.5 Calibrating Static Elastic and Rock Strength Properties

After calculating the dynamic data, static elastic and rock strength properties need to be estimated either using core or using available correlation from the literature. In the literature review section, I summarized of the available correlations to estimate Young's Modulus, UCS and Friction Angle. Table 9, 10 and 11 summarizes the statistical error measurement for the different methods for estimating Young's Modulus, UCS and Friction Angle respectively.

Table 9: Statistical Error Comparison for YM Estimation

Method Name	AARE	EMAX	ESt.D
Morales	286%	620%	147%
John Fuller	37%	70%	18%
Morals Mod	41%	140%	44%

Table 10: Statistical Error Comparison for UCS Estimation

Method Name	AARE	EMAX	ESt.D
Rzhevesky	30%	55%	25%
Plum Clay	110%	162%	37%
Plump Grain	40%	74%	27%
Horsrud	210%	287%	53%
Plump Upper Bound	108%	186%	61%
Plump Shear	63%	123%	55%

Table 11: Statistical Error Comparison for Friction Angle Estimation

Method Name	AARE	EMAX	ESt.D
Weingarten	20%	34%	7%
GR Cutoff	6%	11%	4%

As Shown in Tables 9, 10 and 11 the statistical error in estimating YM, UCS and FANG is high and will make any further calculation for the MEM unreliable. Therefore, an attempt to utilize available core data to construct local correlations for the above-mentioned elastic and rock strength properties was conducted.

The relationship between dynamic YM derived from log data and static YM from multi-stage tri-axial tests was conducted. 8 selected representative core plug data were used to eliminate outliers. Figure 19 shows the best linear fit through the cross-plot data. The data was fitted with the below linear equation with regression factor value of 0.87.

$$YM\_DYN = 0.9196 * (YM\_STA) + 3.5359 \quad (4.8)$$

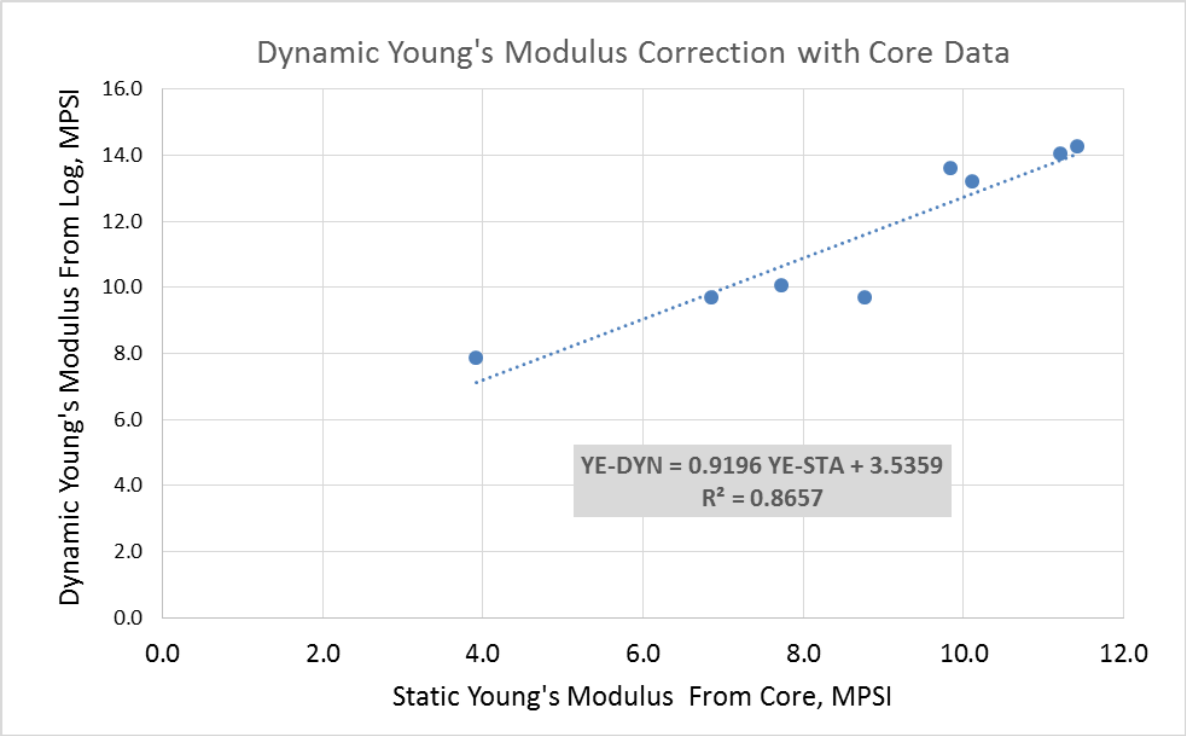

Figure 19: Linear Best fit through cross plot of dynamic YM derived from log data and static YM from multi-stage tri-axial tests for selected core plugs

The relationship between dynamic PR derived from log data and static PR from multi-stage tri-axial tests from. 8 selected representative core plugs were used to eliminate out layers. Figure 20 shows the best linear fit through the cross-plot. The data was fitted with the below linear equation with regression factor value of 0.83.

$$YM\_DYN = 0.189 * (YM\_STA) + 0.348 \qquad (4.9)$$

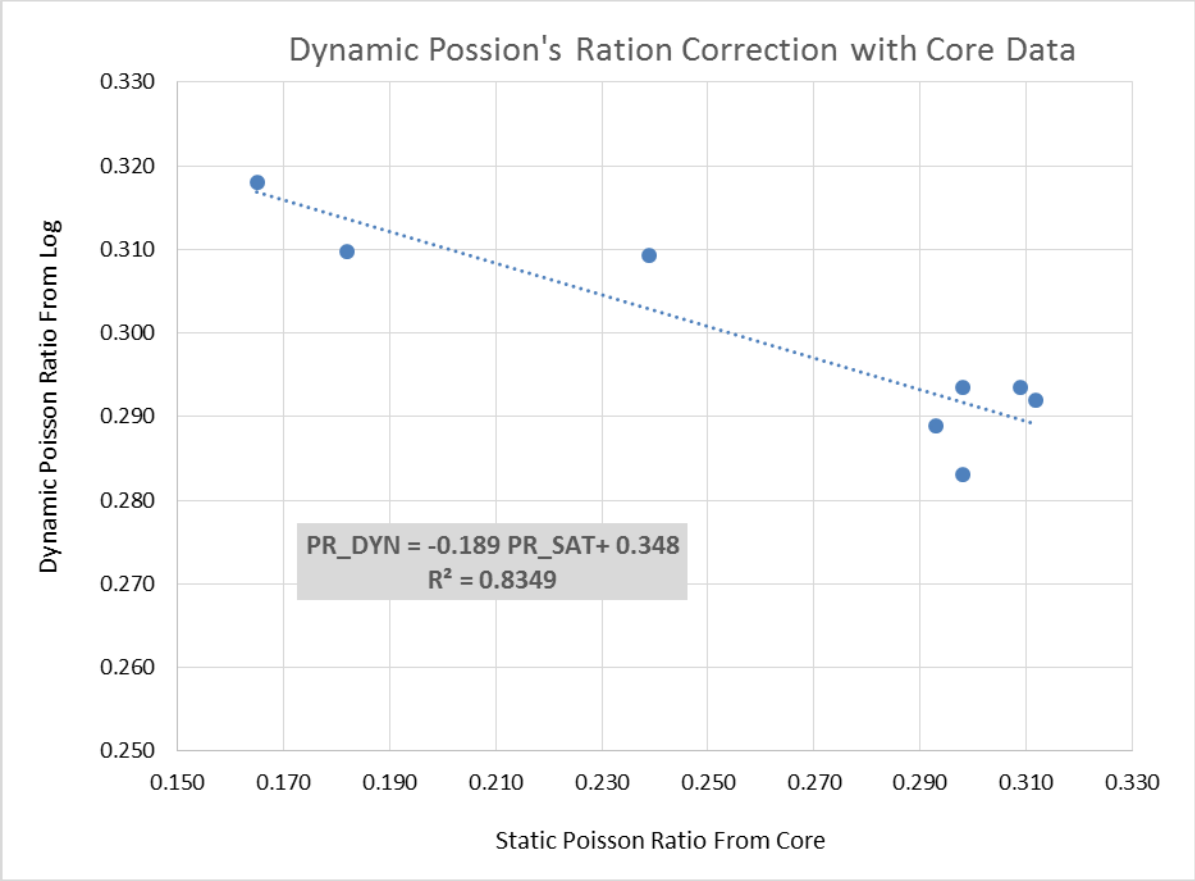

Figure 20: Linear Best fit through cross plot of dynamic PR derived from log data and static PR from multi-stage tri-axial tests for selected core plugs

The relationship between bulk densities derived from log and determined UCS from multi-stage tri-axial tests, 18 selected representative core plugs were used to eliminate outliers. Figure 21 shows the best linear fit through the cross-plot. The data was fitted with the below linear equation with correlation coefficient value of 0.85.

$$UCS = 12{,}825 * \rho\_LOG - 19{,}895 \qquad (4.10)$$

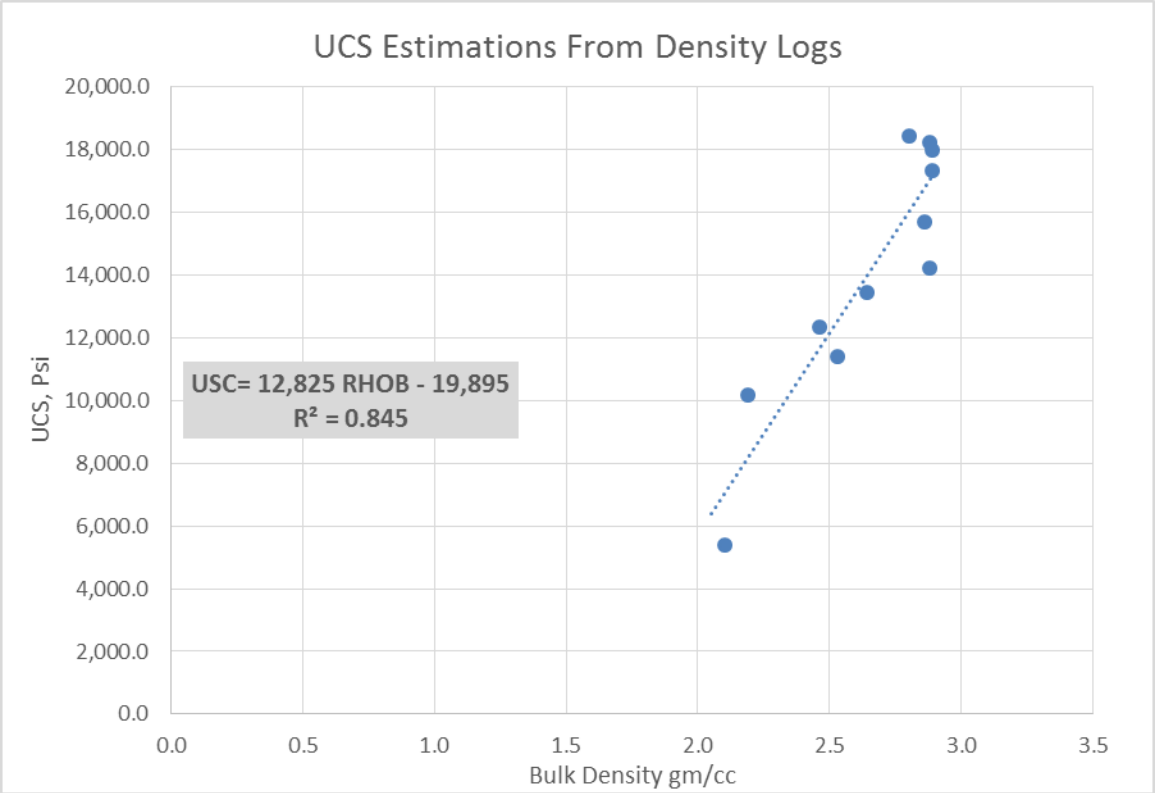

Figure 21: Linear Best fit through cross plot of density log data and UCS measurement from multi-stage tri-axial tests for selected core plugs

The relationship between bulk density from log and FANG from multi-stage tri-axial tests, based on 7 selected representative core plugs to eliminate outliers. Figure 22 shows the best linear fit through the cross-plot data. The plot shows linear equation with correlation coefficient value of 0.89.

$$FANG = 17.489 * \rho\_LOG - 5.1471 \qquad (4.11)$$

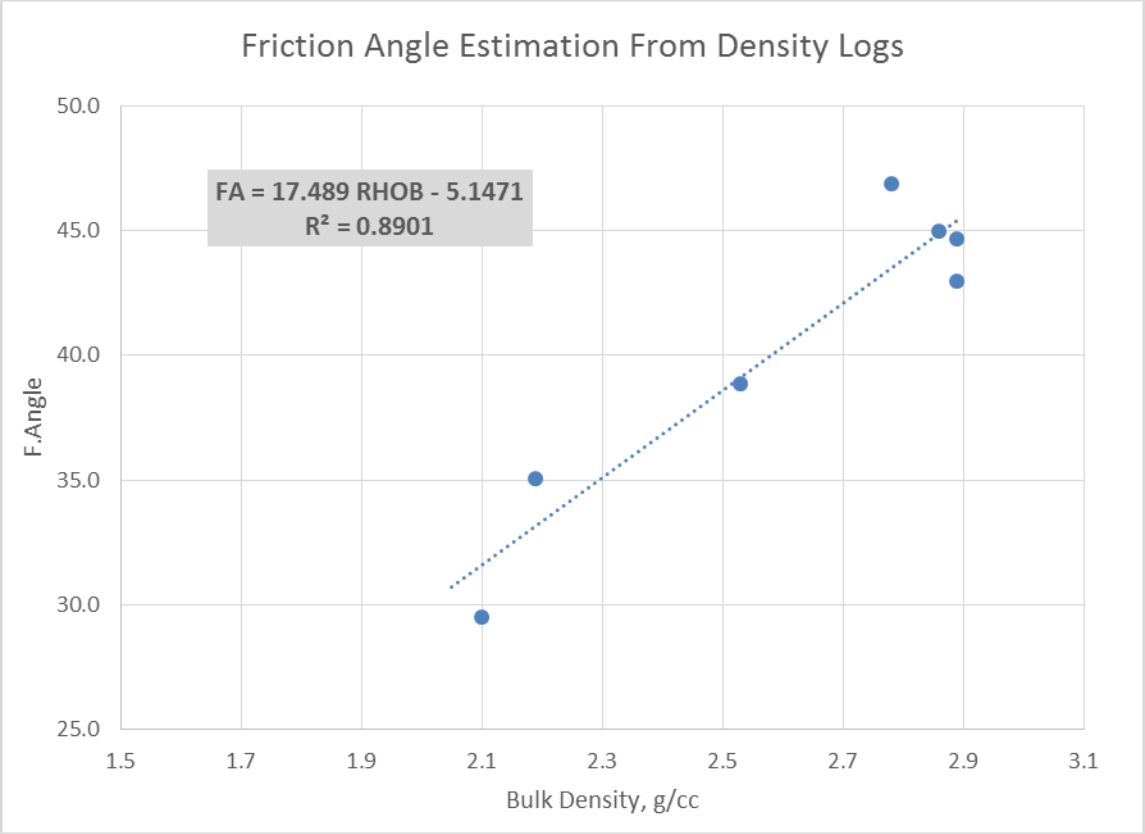

Figure 22: Linear Best fit through cross plot data of dynamic YM derived from log data and static YM from multi-stage tri-axial tests for selected core plugs

4.6 Horizontal Stresses

There few methods reported in the literature for estimating the horizontal stresses. The first method is the Mohor-Coulomb method where the horizontal stress is calculated as function of shear strength and normal effective stress. The second method utilizes the elastic

properties such as, Young's Modulus, Possion Ratio, Biot coefficient….etc. in order to estimate the values of the maximum and minimum horizontal stresses.

4.7 Mohr-Coulomb Stress Model

Mohr-Coulomb Stress Model is a failure model that gives a relationship between two principal stresses if the formation is at failure. The model assumes that the maximum in-situ shear stress is governed by the shear strength of the formation, which is characterized by the Mohr-Coulomb failure criterion. The model is not limited to any specific deformation mechanism or principal stress direction. Therefore, it can be applied to sedimentary basins subjected to either active tectonic compression or extension. Assuming that the vertical stress is the principal stress, the limits of horizontal stresses in the stress domain are the lower limit of minimum horizontal stress, and the upper limit of maximum horizontal stress. Both are obtained from the Mohr-Coulomb Stress Model.

Mohr Circle Horizontal Stresses Calculation Algorithm

According to different tectonic plate movements, you can define three stresses regimes. These stresses regimes are associated with the all classic fault regimes with the most common are thrust and normal fault regimes.

Thrust fault regime

$$\sigma_H > \sigma_h > \sigma_v$$

In this case, the maximum principal stress and minimum principal stress is the vertical stress. The maximum horizontal stress can be estimated using the following equation.

$$\sigma_H = tan^2\left(\frac{\pi}{4}+\frac{\theta}{2}\right)\times(\sigma_v - K\,P_P) + KP_P \qquad (4.12)$$

K Is a factor defined as the ratio between Tensile Strength and UCS approximately 10% .

For normal fault regime:

$$\sigma_V > \sigma_H > \sigma_h$$

In this case, the vertical stress is the major principal stress and minimum horizontal stress is the third principal stress from the following equation:

$$\sigma_h = \frac{(\sigma_v - K\,P_P)}{tan^2\left(\frac{\pi}{4}+\frac{\theta}{2}\right)} \times + KP_P \qquad (4.13)$$

Poro-Elastic Horizontal Strain Model

Poro-Elastic Horizontal Strain Model is the most generally used method for horizontal stresses determination. The Poro-Elastic Horizontal Strain Model can be expressed using Static Young's modulus, Poisson ratio, Biot's constant, overburden stress, and pore pressure. The maximum and minimum horizontal stresses in this method can be calculated using equation; (eq. 4.14 & 4.15).

$$\sigma_H = \frac{v}{1-v}\,\sigma_v - \frac{v}{1-v} + \alpha P_P + \frac{E}{1-v^2}\varepsilon_h + \frac{vE}{1-v^2}\varepsilon_H \qquad (4.14)$$

$$\sigma_h = \frac{v}{1-v}\,\sigma_v - \frac{v}{1-v} + \alpha P_P + \frac{E}{1-v^2}\varepsilon_H + \frac{vE}{1-v^2}\varepsilon_h \qquad (4.15)$$

Due to the availability of core data to calibrate the elastic and rock strength properties in this study, the Poro-Elastic Horizontal Strain Model was the model of choice used for horizontal stress approximately. The minimum and maximum principal horizontal strain, ε_H and ε_h are calibration parameters were developed from previous geomechanical work and estimated at value of 0.001 due to the lack of extended Leak-Off Test (ELOT) results. In addition to maximum and minimum horizontal stresses, the wellbore instability analysis includes Critical Mud Weight for kick (Kick Limit) which is an eruption or flow of drilling mud from a wellbore resulting from the entry of formation fluids, oil, gas, or water into the borehole. Such entry occurs when the pressure in the borehole does not counterbalance the pressure in permeable formation. The Loss Circulation limit is Critical Mud Weight for mud loss, which is equal to the minimum in-situ principal stress. Figures 22 and 23 shows the safe MW widow resulting from the usage of the Poro-Elastic Horizontal Strain Models for Well-A and Well-F data. The following are the displayed limits on both figures the critical mud weight for kick (Kick limit), loss circulation limit (minimum in-situ principal stress) and used MW to drill the reservoir section, all in ppg.

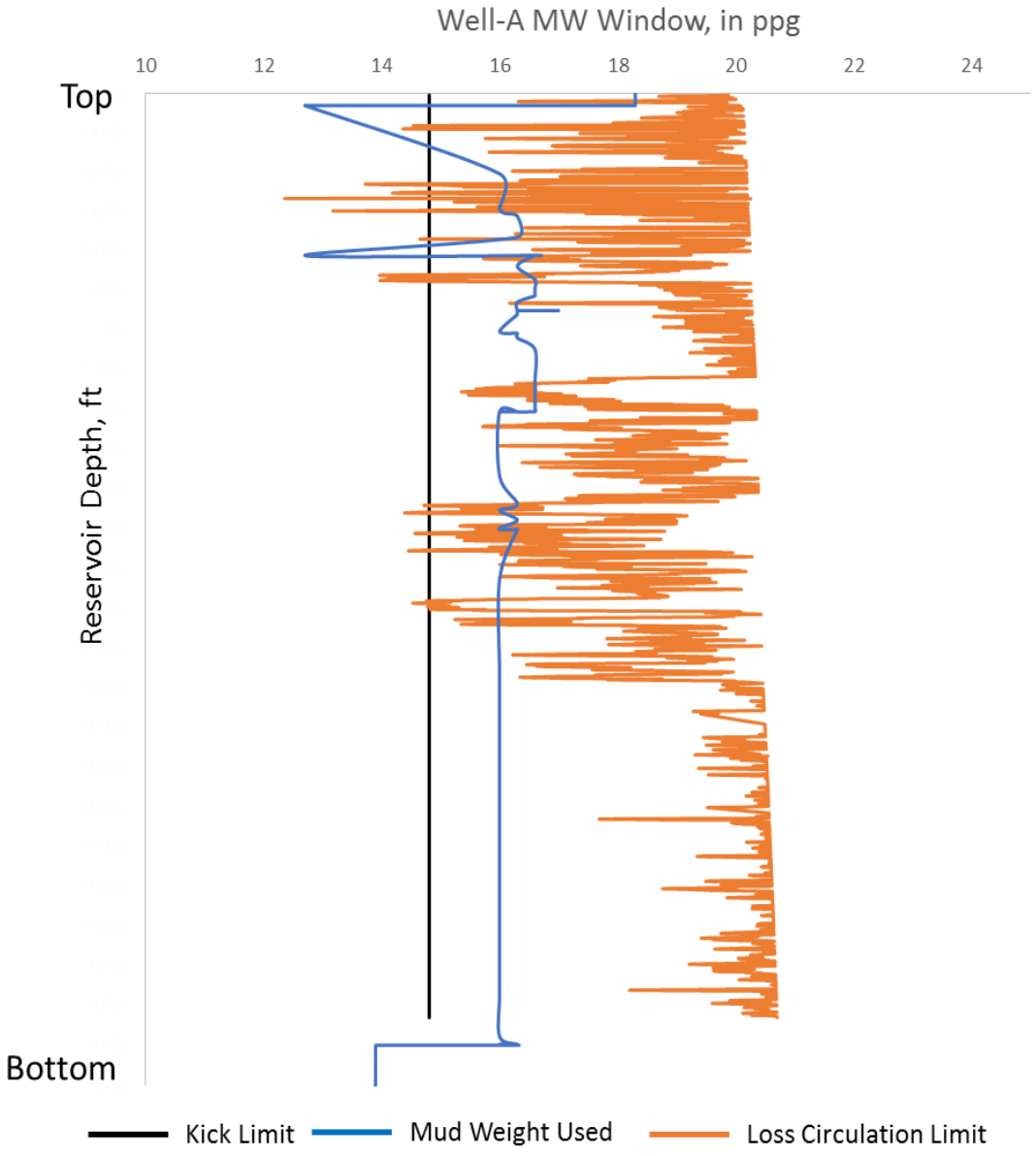

Figure 23: Safe Mud weight window and actual mud weight used for Well A

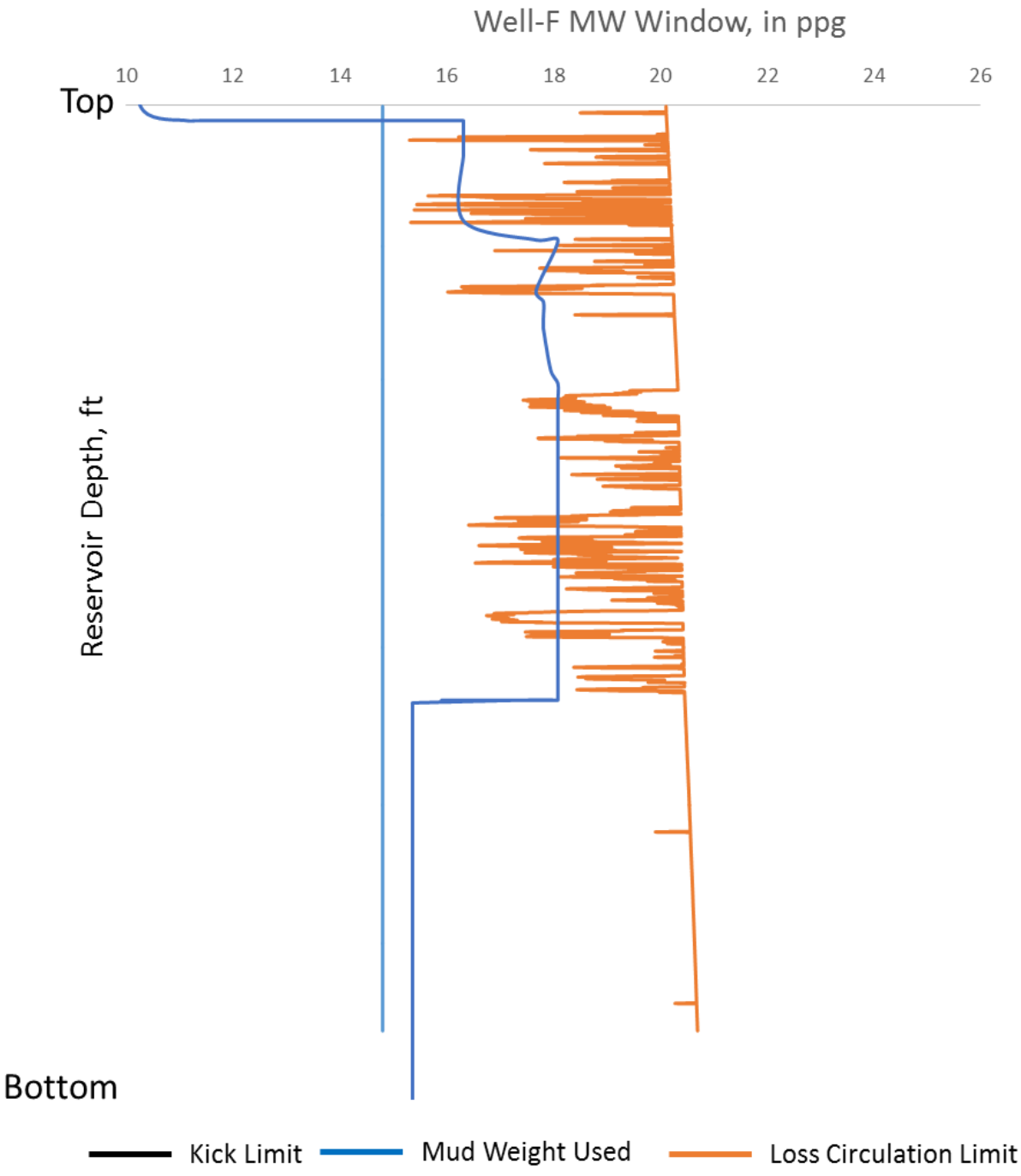

Figure 24: Safe Mud weight window and actual mud weight used for Well F.

4.8 Loss circulation Data Interpretation

After calculating the safe mud weight window for the wells considered in this study, a detail review for the loss circulation events in will be attempted order to deduce reason behind their occurrence. This will be utilizing the calculated safe mud weight windows in the previous chapter. The events where the safe mud weight window was violated will be highlighted. In the incidents were the safe mud weights were followed and loss circulation happened, data such image logs and core data if applicable will be used to give rise for such events.

4.9 Well-A and Well-F Loss Circulation Event Analysis

The below table shows the reported events where loss circulation occurred in Well-A and Well-F highlighted in previous chapter. The upper and lower limit for the safe mud weight window are also included and if the used mud weight is in violation of the previously calculated safe mud weight window. Table 12 and Table 13 shows the event of loss circulation against the calculated Wellbore Stability Safe Mud weight window calculated in pervious chapters along with the actual mud weights used in drilling the section per drilling activities morning reports.

Table 12: Qualitative Analysis of Safe Mud weight window (SMW) and actual mud weight used for Well A at Loss Circulation Events Depth.

Depth MD	Used MW PPG	Lost Volume BBL	Avg. Loss Rate BBL/Day	Summary of Safe MW Observation
11010	17	102	4	A violation for SMW in (±) 20 ft
11302	17	300	13	No Clear Violation for SMW
11724	16	250	10	A violation for SMW in (±) 20 ft
11990	16	50	2	A violation for SMW in (±) 20 ft.
12775	16	50	2	No Clear Violation for SMW

Table 13: Qualitative Analysis of Safe Mud weight window (SMW) and actual mud weight used for Well F at Loss Circulation Events Depth.

Depth MD	Used MW PPG	Lost Volume BBL	Avg. Loss Rate BBL/Day	Summary of Safe MW Observation
12,527	16	658	7	No Clear Violation for SMW
13,103	16	906	10	No SMW calculation as section was not logged

Figures 25 up to Figure 30 shows the safe MW widow for the tabulated intervals above from both Well-A and Well-F data. The limits the MW window include, the minimum and

maximum horizontal stress, the kick limit and the loss circulation limit all in ppg as previously discussed in previous chapters.

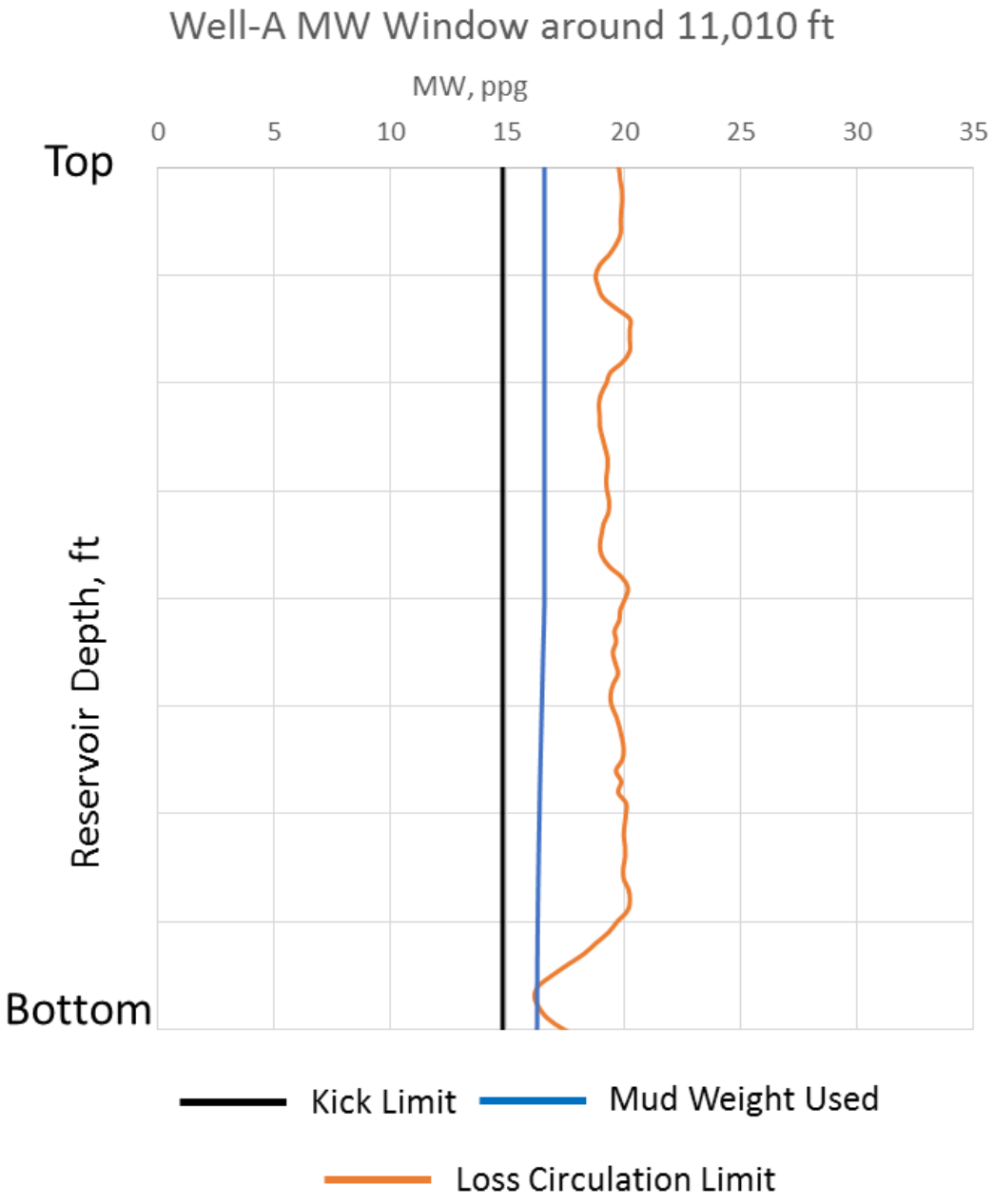

Figure 25: Safe Mud weight window and actual mud weight used for Well-A along around loss circulation event at 11,010 ft.

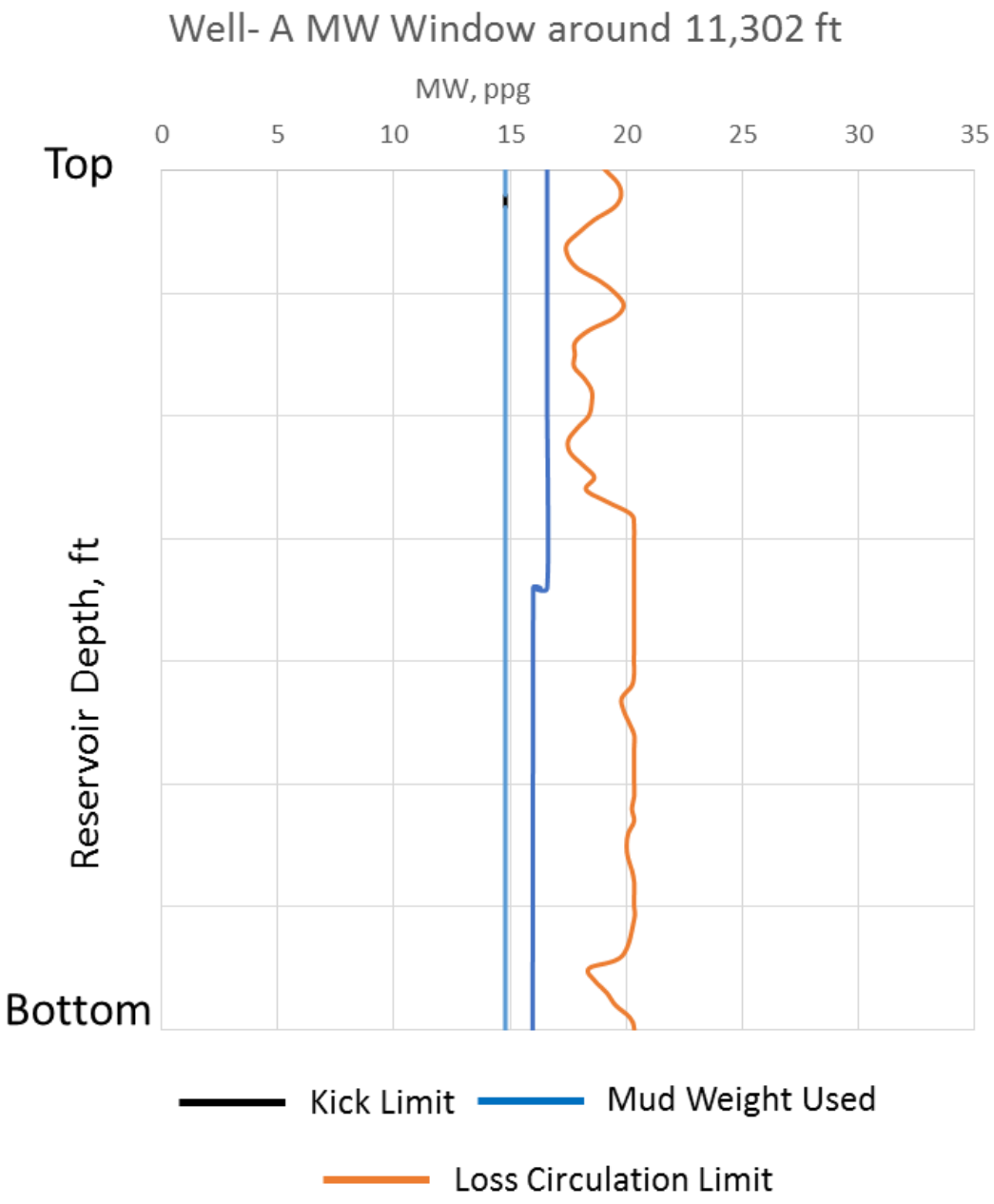

Figure 26: Safe Mud weight window and actual mud weight used for Well-A along around loss circulation event at 11,302 ft.

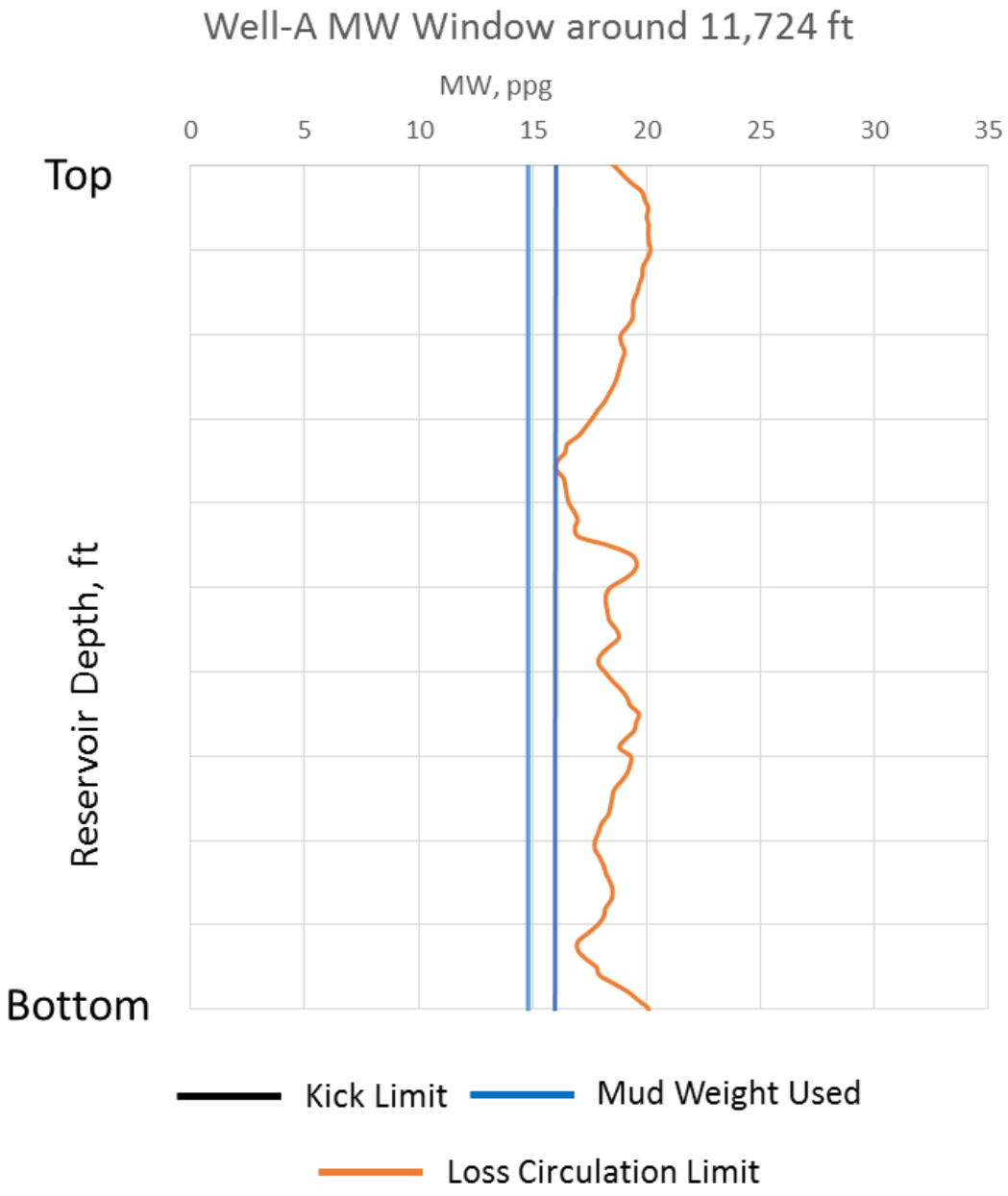

Figure 27: Safe Mud weight window and actual mud weight used for Well-A along around loss circulation event at 11,724 ft.

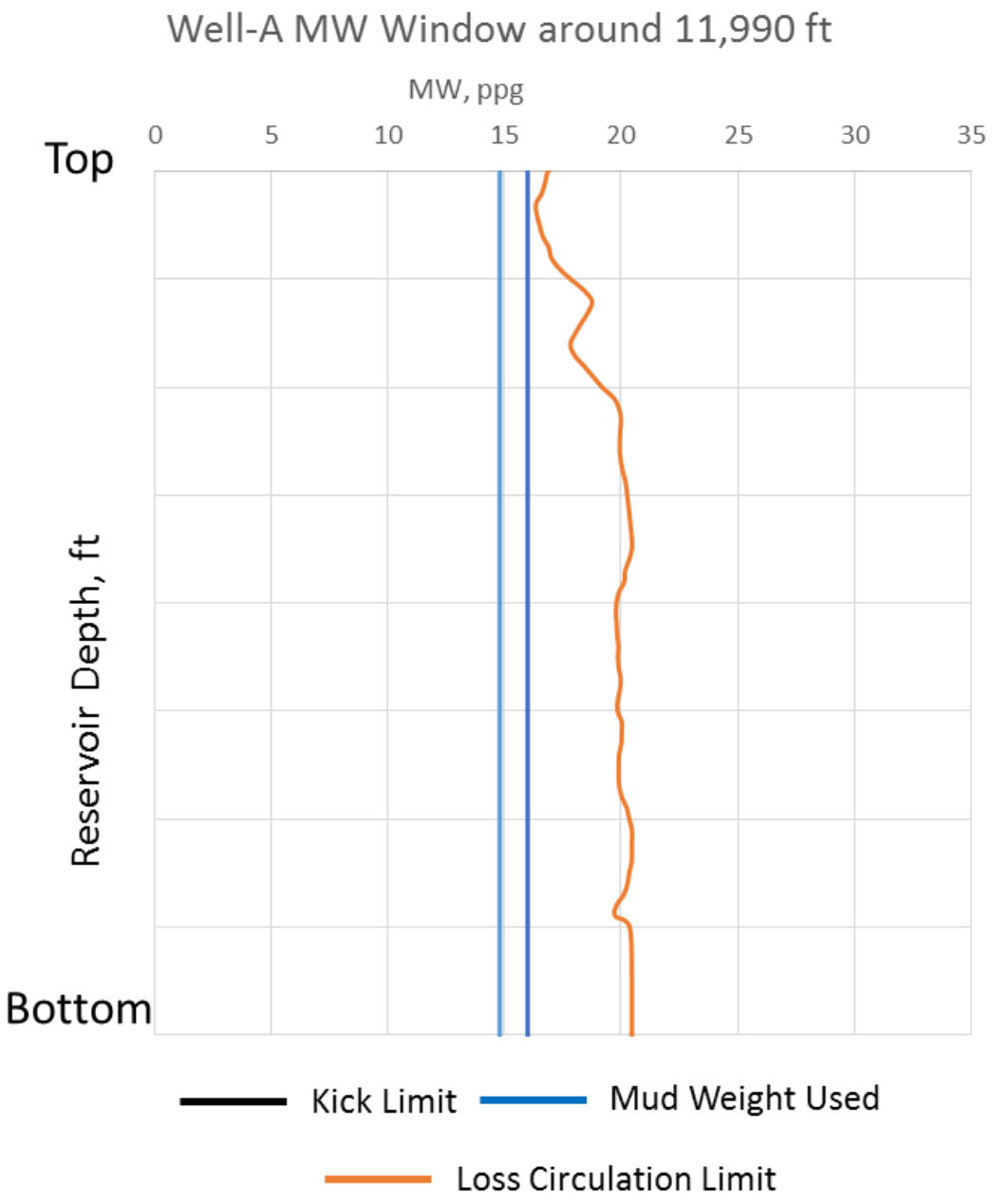

Figure 28: Safe Mud weight window and actual mud weight used for Well-A along around loss circulation event at 11,990 ft.

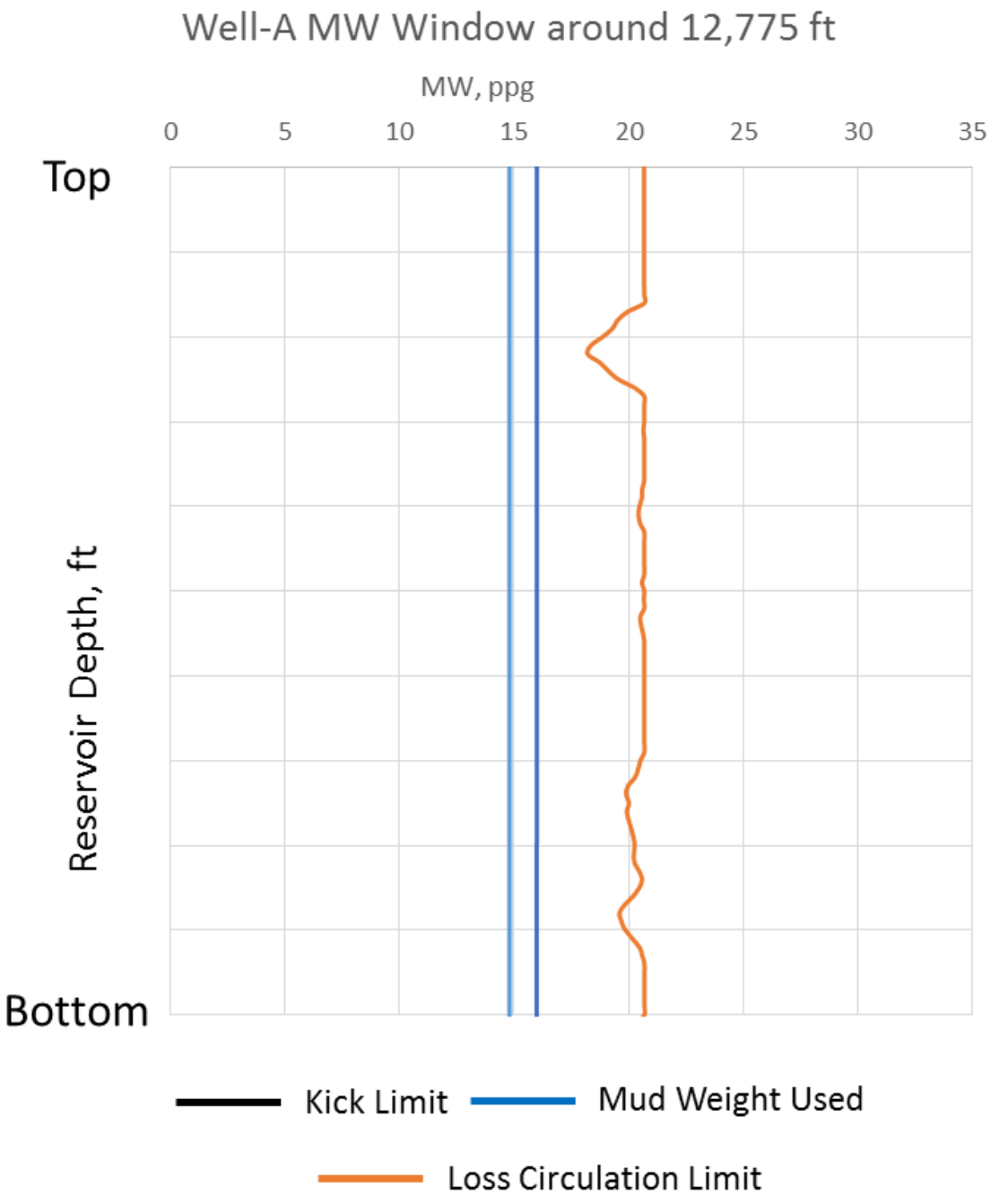

Figure 29: Safe Mud weight window and actual mud weight used for Well-A along around loss circulation event at 12,775 ft.

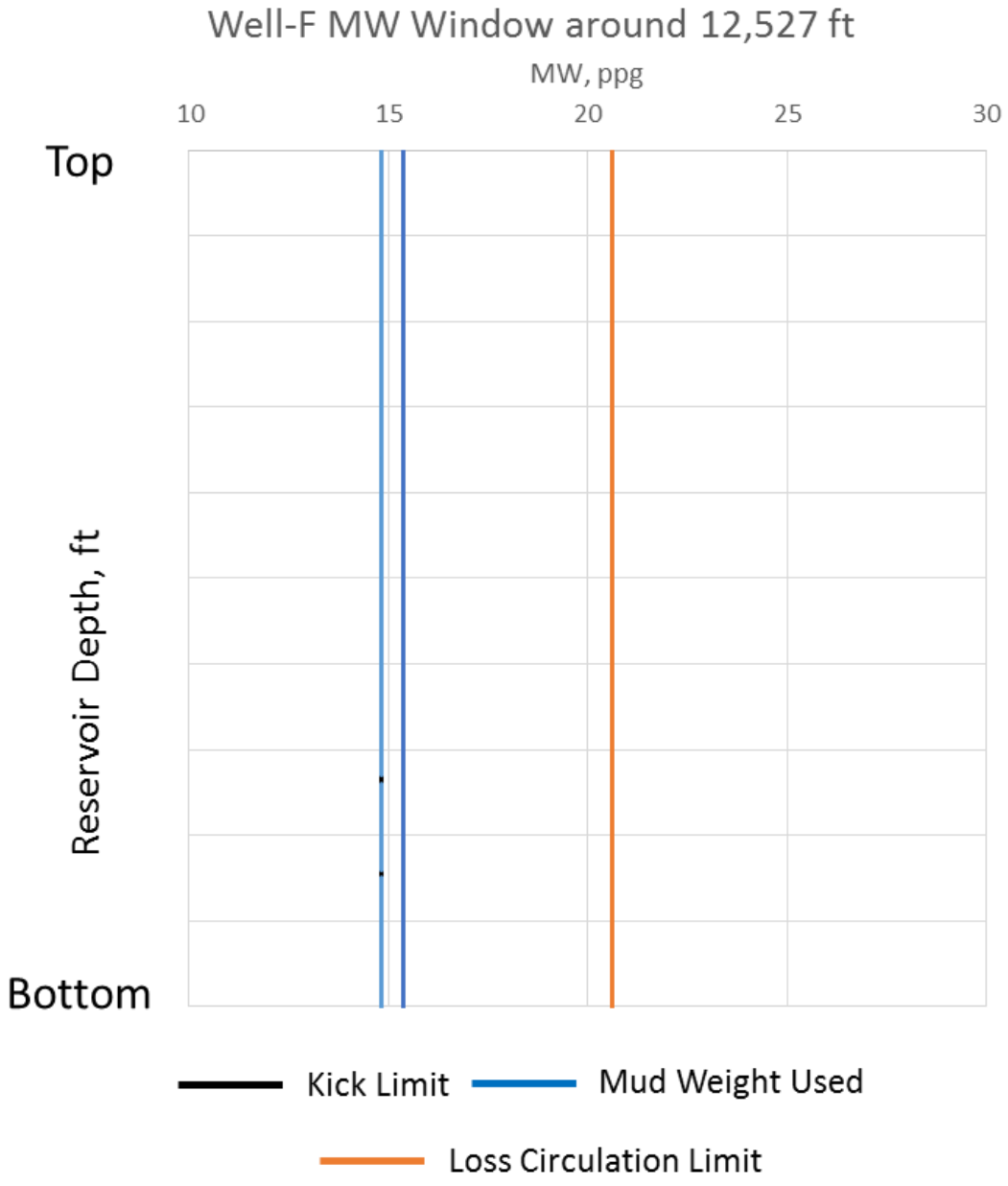

Figure 30: Safe Mud weight window and actual mud weight used for Well-F along around loss circulation event at 12,527 ft.

Following the safe MW window analysis, it was clear that wellbore stability events represented in the loss circulation depths and volumes can be classified into two categories:

1. Mud weight used exceeded calculated Safe Mud Weight Window, which were experienced at four events (at depths 11,010 ft., 11,724 ft., 11,990 ft. and 12,275 ft.). In those cases, the high overbalance used in drilling the section resulted exceed the loss circulation limit and possibly initiate drilling induced tensile fractures. Those events were to be avoided if a pre-drilling wellbore stability model was used to guide the drilling mud weight design. The loss circulation event happened at 11,724 ft. was the major event with around 1,500 bbl. was lost at that depth. Available Image logs across the investigation interval had confirmed a presence of drilling induced tensile fractures.

2. Mud weight used fall within calculated Safe Mud Weight Window, which were experienced at several events (at depth 11,302 ft. in well-6 and 12,527 ft. and 13,103 ft. in Well-F). In those cases, the overbalance used drilling this section was within the safe limit and it is highly unlikely the mud weight used will initiate drilling induced fractures. Those events do not have any justification in terms the wellbore stability model. With the heavily fractured nature of the reservoir, a thorough analysis of the available core and image logs and pressure transient data will be used to deduce if the loss circulation happened because of the natural fracture existence or not. Available Image logs across the investigation interval had confirmed a presence of natural fractures.

4.10 Presence of Natural Fractures from Image Log Data

In order to confirm the presence of natural fractures in the reservoir under study a holistic review in order to determine if the presence of natural fractures at that depth had contributed to the loss circulation event occurred or not. Interpreted acoustic Image Logs was only the available data attribute for analyzing the existence of fractures at those depths. No core was collected across these intervals in order to visually characterize the fractured nature of the reservoir in those depths. Figure 31 to Figure 36 shows the interpretation of the image logs captured at the depth of the loss circulation events in Well-A and Well-F while no available image logs for Well-A at a depth of the 5th event at 12,775 ft.

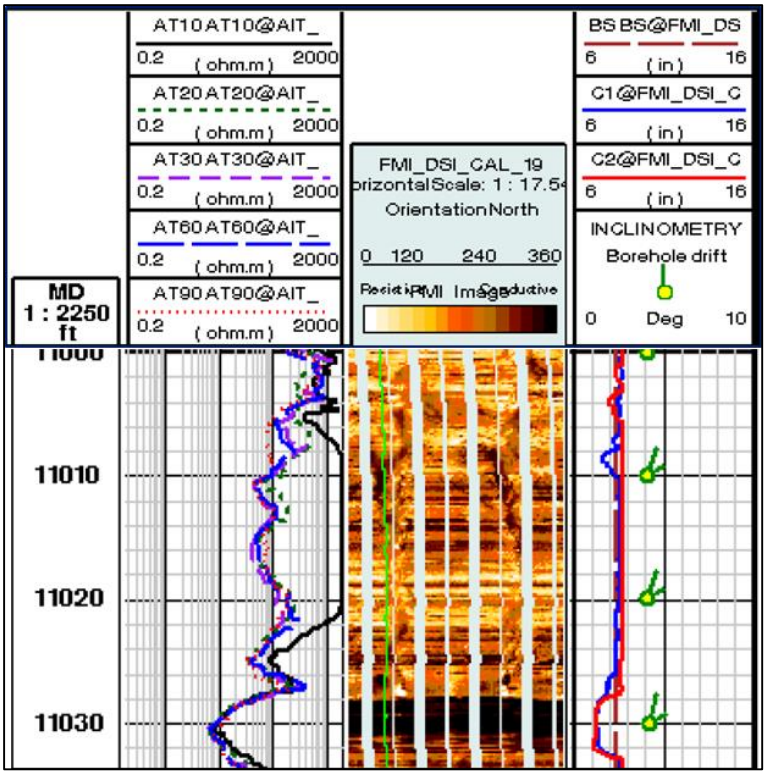

Figure 31: Interpreted Well-A Image Log data around the depth 11,010 ft. showing induced fractured at the investigation depth.

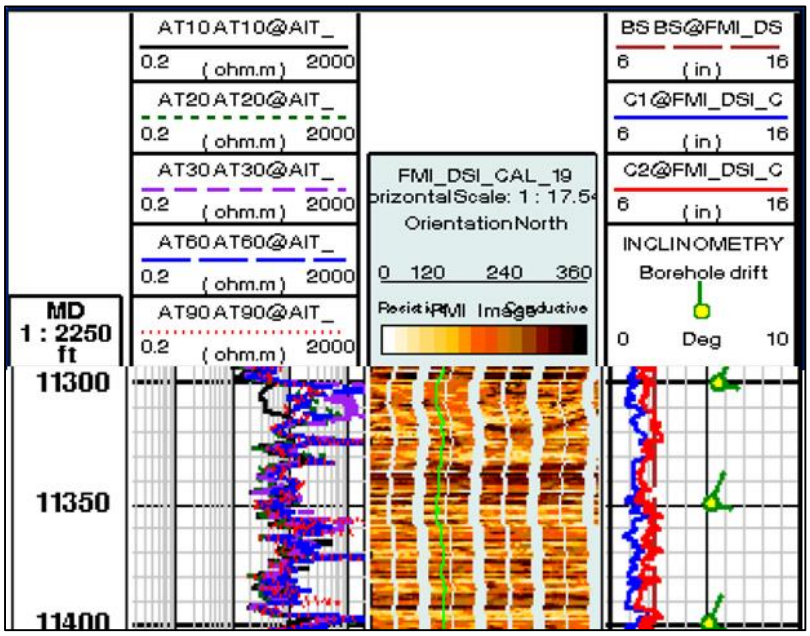

Figure 32: Interpreted Well-A Image Log data around the depth 11,302 ft. showing high density of natural fractures at the investigation depth.

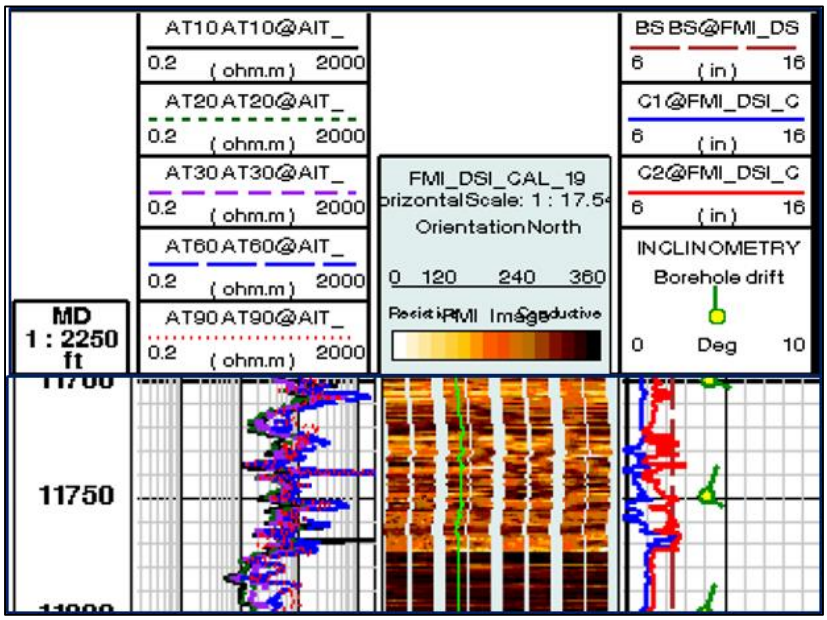

Figure 33: Interpreted Well-A Image Log data around the depth 11,724 ft. showing induced fractures at the investigation depth.

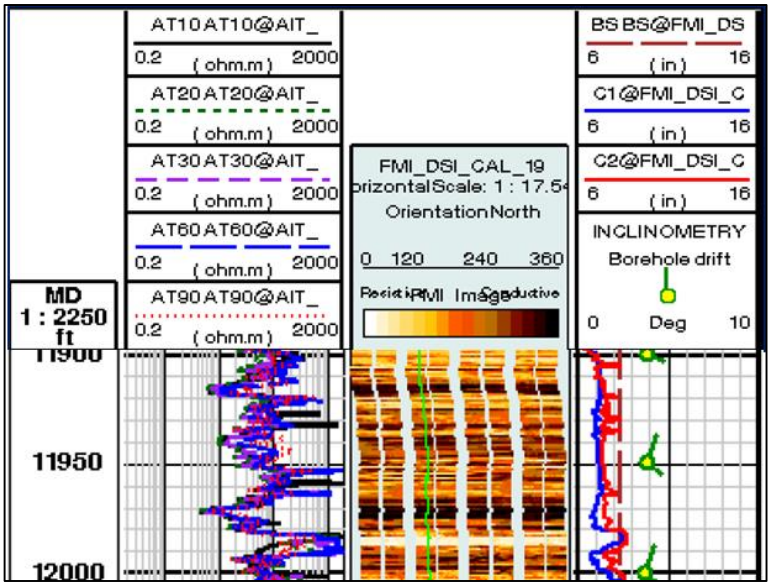

Figure 34: Interpreted Well-A Image Log data around the depth 11,990 ft. showing induced fractures at the investigation depth.

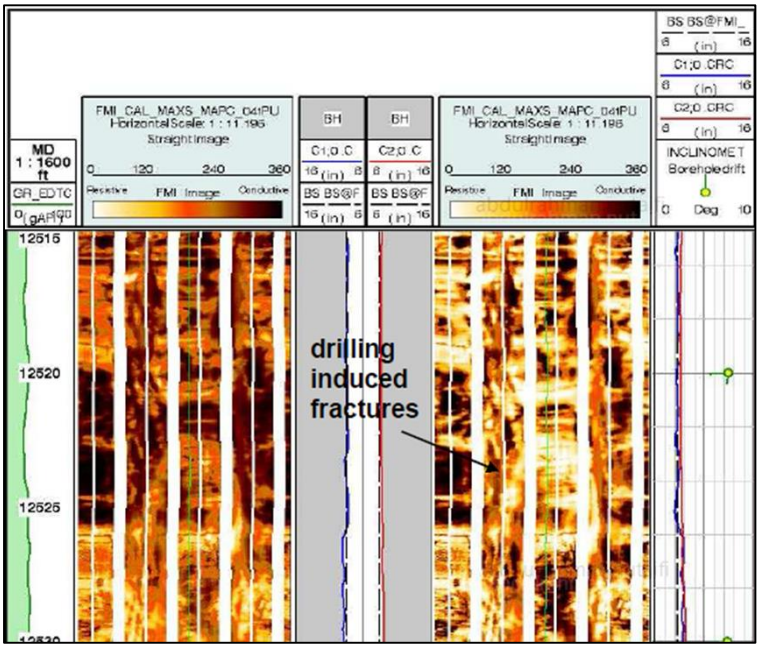

Figure 35: Interpreted Well-F Image Log data around the depth 12,527 ft. MD showing induced fractures at the investigation depth.

4.11 Loss Circulation Management in Fractured Reservoirs

As deduced in previous sections, the contribution of natural fractures into loss circulation is significant. From Well-A and Well-F data, the loss circulation volume in natural fracture is significantly higher than those in induced fractures. This due to the fact that induced fractures geometry is impacted by the drilling parameters which are adjusted once the loss circulation occurs to control the fluid losses. Figure 36 shows a comparison between the lost circulation volumes between the two types of fractures deduced from Well-A and Well-F Data.

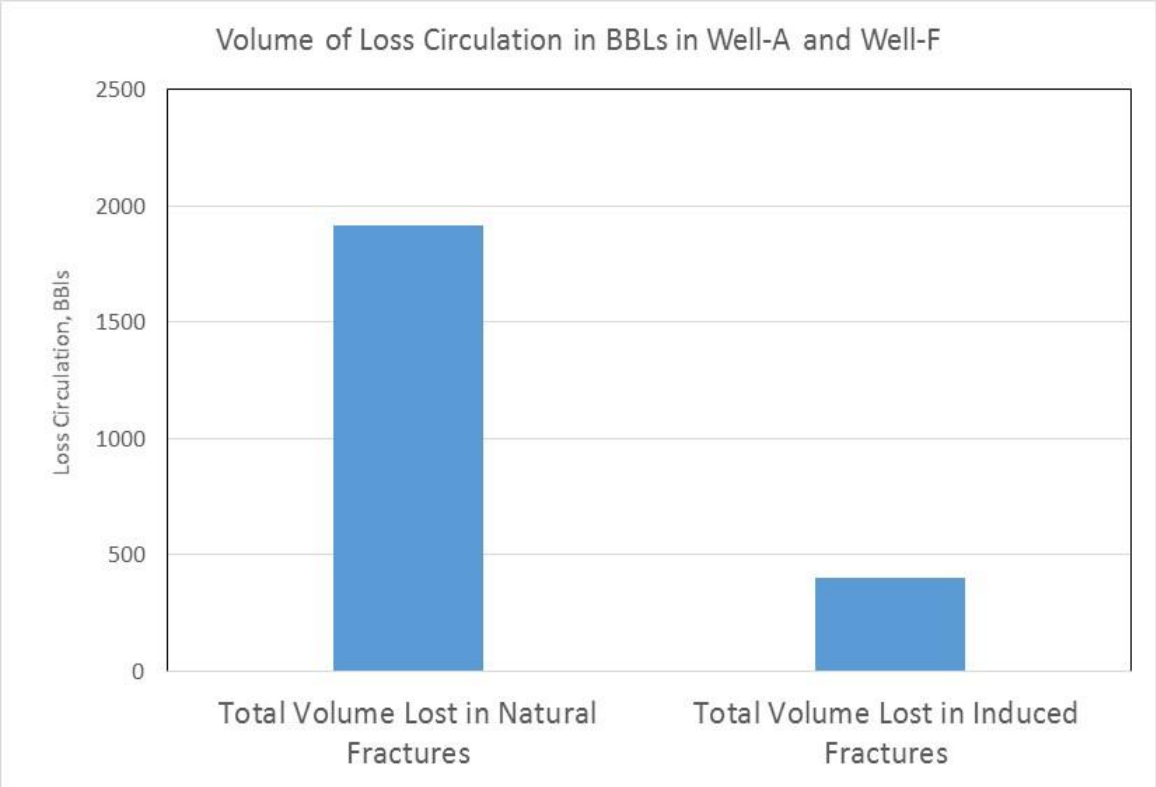

Figure 36: Volume of Loss Circulation in BBLs in Well-A and Well-F

To control the loss circulation several techniques and methods can be deployed. The first is to include special loss circulation material (LCM) into the mud recipe that will plug to

an extent the fractures and stop the seepage of fluid into them. There are range of LCMs materials that varies depending on what the application its deployed for both for non-reservoirs or reservoirs sections. In the case of non-reservoirs, it can be fairly stated that the range of LCMs is broad as damage is not of concern (Savari, 2016). However, LCM selection if losses happen across reservoir need to be non-damaging, degradable or can be dissolved through small stimulation jobs. With such requirements, the choice of LCMs in case of losses in a reservoir can be very limited. In the area under study the choice to counter the loss circulation was Calcium-carbonate-based "calcium chips' however showed limitation as excessive volumes of LCM were used in some well loss circulation events and was not fully effective in stopping the losses. Different techniques, such as managed-pressure drilling and underbalanced drilling, are also being used to control losses across the reservoir section as they are not damaging (methods such as cementing the section of loss circulation is a practice that will not apply to reservoir section as its plugs the formation completely and not soluble in any acid.

Managed Pressure Drilling (MPD) is a good option where there is a very tight pressure window between pore and fracture gradients. In the managed pressure drilling or mud cap drilling a pressure is applied on the wellbore through surface pumps to apply additional on fluid column to make control the hydrostatic pressure on the reservoir.

Underbalanced Drilling (UBD) eliminates the lost circulation problem because mud weight is designed to be below pore pressure. Also under balance drilling is often used to reduce the hydrostatic pressure below formation pressure and drill the well while it is flowing to the surface through either flaring the produced gas or connect it to a production

facility.

Casing while Drilling also provide an aggressive loss circulation stop mechanism by which casings are run and the fractures are cased instantly by plaster the formation cuttings to into the fractures. However open fractures might provide source of hydrocarbon formation fluid to migrate and cause pressure in the Casing Casing Annuli (CCA) or Tubing Casing Annuli (TCA). However, with the risks associated both the MPD, UBD and Casing while drilling in the high pressure and high temperature offshore environments prevented deploying these methods to control the losses.

4.12 Fractures Geometry Prediction from Loss Circulation Data

Liétard [1999, 2002] was one of the early researchers looking into the loss circulation data to deduce fracture geometry from it. He considered mud-flow invasion into a fracture defined as a hollow cylindrical aperture of height w and internal as shown in Figure 37, where r_w is the wellbore radius and $(r_s)_{max}$ is the maximum invasion radius. He assumed rheological behavior of the non-Newotonian drilling mud to be modeled as Bingham Fluid.

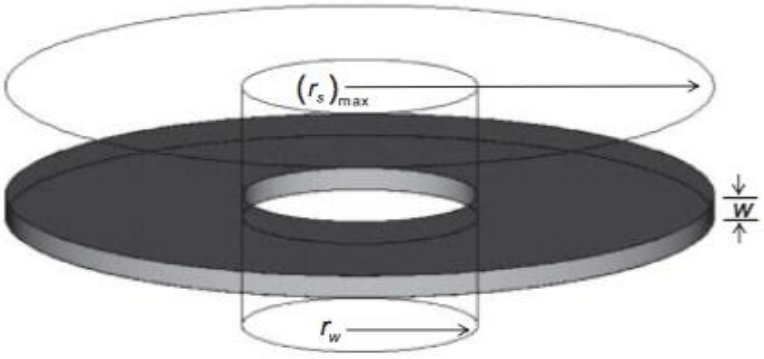

Figure 37: Volume of Loss Circulation in BBLs in Well-A and Well-F

In a following work, Huang [2011] deduced a formula, testing by the data from Liétard work to estimate the width of the fracture as in equation 5.1.

$$w = \left[\frac{9\,(V_m)_{max}/\pi}{(\frac{\Delta p}{\tau_y})^2} \right]^{1/3} \qquad (5.1)$$

Where, w is the fracture width in meters $(V_m)_{max}$ is the total mud lost in the section in BBL, $\frac{\Delta p}{\tau_y}$ is the overburden pressure used to drill the section in psi. Applying this formula to the loss circulation data from Well-A and Well-F, Table 14 and 15 shows the expected fracture width in micro meters estimated from equation 5.1.

Table 14: Well-A expected fracture width from drilling and loss circulation data.

Depth	Used MW	Overburden Pressure	Lost Volume	Estimated Fracture Width
MD	PPG	Psi	BBL.	Micro Meter
11,010	17	653	102	42.39
11,302	17	911	300	48.64
11,724	16	674	250	55.93
11,990	16	896	50	27.07
12,775	16	629	50	34.27

Table 15: Well-F expected fracture width from drilling and loss circulation data.

Depth	Used MW	Overburden Pressure	Lost Volume	Estimated Fracture Width
MD	PPG	Psi	BBL	Micro Meter
12,527	16	422	658	105.48
13,103	16	902	906	70.79

4.13 Natural Fractures Reservoirs Challenges and Management

Extensive research was directed into the detection, characterization and modeling of the natural fractures in the past three to four decades as we have seen in previous sections. However, accumulated knowledge of how to better develop and manage fractured reservoirs is still limited. The importance of the natural fractured reservoir lay in the production performance contribution of the natural fractures which contribute to the prolific well performance and thus reducing development drilling requirements specially in gas field development. In the studied field, the natural fracture contribution to well performance was evident through comparing the flow capacity (KH) from the pressure trainset behavior for conducted pressure Build Up (BU) tests and the KH from matrix core plugs' data. So, it is critical not to avoid these fractures and ensure that they are intersected and kept open to assure contribution to wellbore gas influx. This is key for increasing the ultimate recovery for dry gas reservoirs. However, if fractured reservoirs are poorly managed, especially in oil and rich gas reservoirs, the ultimate recovery of these fields can be greatly reduced due to the changes in Gas-Oil Rations and water production that can

cause serious decline of wells performance. Allan [2003] summarized the impact of natural fractures on increasing the ultimate recovery of nearly 100 oil and gas reservoirs. He also highlighted the best development mechanism and EOR methods that suit each type of reservoirs. The data obtained in his study indicated that ultimate recoveries in fractured reservoirs are somewhat lower than those of many conventional reservoirs. Thomson [1981] highlighted that to manage a fractured reservoir optimally, one needs to establish injection/production scenarios (pressure maintenance strategies, enhanced recovery strategies, pattern orientation, deviated well orientations, and other such scenarios), bypassed zones or compartments need to be predicted, and effective risk-based economic scenarios need to be able to be run. Since the natural fractures are need to maintained undamaged, open hole completions is usually preferred as the completions method (Abdollahi, 2004).

Certainly, well planning is the first step to reduce the associated risk during drilling operation and minimize the exposure to the fractures beyond what will sufficiently contribute to the well performance. Changing the well geometry, if reservoir thickness and permeability permits, from extended horizontal to vertical or moderately deviated wells to reduce intersecting fractures or placing the wells away from areas with excessive high density fractures could reduce the time needed to fight loss circulation or related problems which is one of the main consequence of drilling through natural fractures.

To control the loss circulation several techniques and methods can be deployed. The first is to include special loss circulation material (LCM) into the mud recipe that will plug to an extent the fractures and stop the seepage of fluid into them. There are range of LCMs

materials that varies depending on what the application its deployed for both for non-reservoirs or reservoirs sections. In the case of non-reservoirs, it can be fairly stated that the range of LCMs is broad as damage is not of concern (Savari, 2016). However, LCM selection if losses happen across reservoir need to be non-damaging, degradable or can be dissolved through small stimulation jobs. With such requirements, the choice of LCMs in case of losses in a reservoir can be very limited. In the area under study the choice to counter the loss circulation was Calcium-carbonate-based "calcium chips' however showed limitation as excessive volumes of LCM were used in some well loss circulation events and was not fully effective in stopping the losses. Different techniques, such as managed-pressure drilling and underbalanced drilling, are also being used to control losses across the reservoir section as they are not damaging (methods such as cementing the section of loss circulation is a practice that will not apply to reservoir section as its plugs the formation completely and not soluble in any acid.

Managed Pressure Drilling (MPD) is a good option where there is a very tight pressure window between pore and fracture gradients. In the managed pressure drilling or mud cap drilling a pressure is applied on the wellbore through surface pumps to apply additional on fluid column to make control the hydrostatic pressure on the reservoir.

Underbalanced Drilling (UBD) eliminates the lost circulation problem because mud weight is designed to be below pore pressure. Also under balance drilling is often used to reduce the hydrostatic pressure below formation pressure and drill the well while it is flowing to the surface through either flaring the produced gas or connect it to a production facility.

Casing while Drilling also provide an aggressive loss circulation stop mechanism by which casings are run and the fractures are cased instantly by plaster the formation cuttings to into the fractures. However open fractures might provide source of hydrocarbon formation fluid to migrate and cause pressure in the Casing Casing Annuli (CCA) or Tubing Casing Annuli (TCA). However, with the risks associated both the MPD, UBD and Casing while drilling in the high pressure and high temperature offshore environments prevented deploying these methods to control the losses.

4.14 Observations

Image logs confirmed the presence of natural fractures in the reservoir under study at the depths where no apparent violations to the safe MW window were at depth 11,302 ft. and 12,775 ft. in Well-A and at 12,527 in Well-F. Those evidences confirm that natural fractures contributed to the loss circulation event that occurred. With such, out of the study for the available data, the following can be deduced:

- Safe MW Window which was derived from the 1-D Mechanical Earth Model was violated in several depths resulting in induced fractures that contributed to loss of circulation events.
- Natural fracture's presence confirmed from the image log analysis had contributed into the loss of circulation events in areas where safe mud weight window was not violated.

- For future drilling programs, and if similar reservoir properties to either well-A or Well-F is expected, the safe mud weight window seen from the 1-D MEM should be a good design basis for mud weight across similar reservoir sections.
- It is highly recommended to couple Image logs data and 1-D MEM modeling for all wells if sufficient data is available in order to build similar root cause analysis for all circulation events and use it to build confidence interval for both the neighboring wells or at filed wide scale.
- Several Mitigation methods to control loss circulation are developed for both reservoir and non-reservoir sections.
- For the area in this study, which is high pressure high temperature environment, only control with LCM material was used as other methods poses high risk.
- Fracture geometry based on literature review can be estimated using drilling and lost circulation data. Width was estimated for Well-A and Well-F lost circulation events.

CHAPTER 5

OBSERVATION ON RELATIONSHIP BETWEEN LOSS CIRCULATION EVENTS AND 3D SEISMIC DATA

Utilizing the analysis carried for the wells Well-A and Well-F in which I identified the type of fractures that contributed to loss circulation events. In this chapter I will try to investigate potential relationships between loss circulation data and other parameters including rock strength and mechanical properties in order to predict such events in future wells where no enough data is available to construct the 1-D Mechanical Earth Model. In this section data from Well-D, Well-E was included next to available data form Well-A and Well-F.

5.1 Loss Circulation Volume Prediction from 3D Seismic' Data

A statistical approach was used to investigate the dependency between loss circulation volume and the rock properties that can be inferred from 3D seismic data. The ratio between shear wave velocity (V_s) and compressional wave velocity (V_p) was selected in the investigation of this work. Values of V_s and V_p were estimated at the depth of the loss circulation events using the available open hole logs (Time domain for both shear and compression waves). Vp and Vs was cross-plotted against the loss circulation data. The ratio between the shear and compression wave velocities was then computed and used in the investigation. Figure 38 and Figure 39 shows the cross plot between the shear velocity (Vs) and compression velocities (Vp) against loss circulation data (Correlation Coefficient

is 0.7 and 0.3 respectively). There is no clear trend between these quantities that can be used to establish a relationship. However, by using the ratio Vp/Vs, a linear best fit was estimated to have a regression error of 0.82 which can be used to suggest the relationship between loss circulation magnitude and Vp/Vs ratio captured from log data. Thus, the Vp/Vs ratio can be computed from 3D seismic data which makes predicting the circulation zones feasible. The Interpreted cross-plot between loss circulation volume (BBL) and ratio between compression and shear velocities (Vp/Vs) is shown in Figure 40.

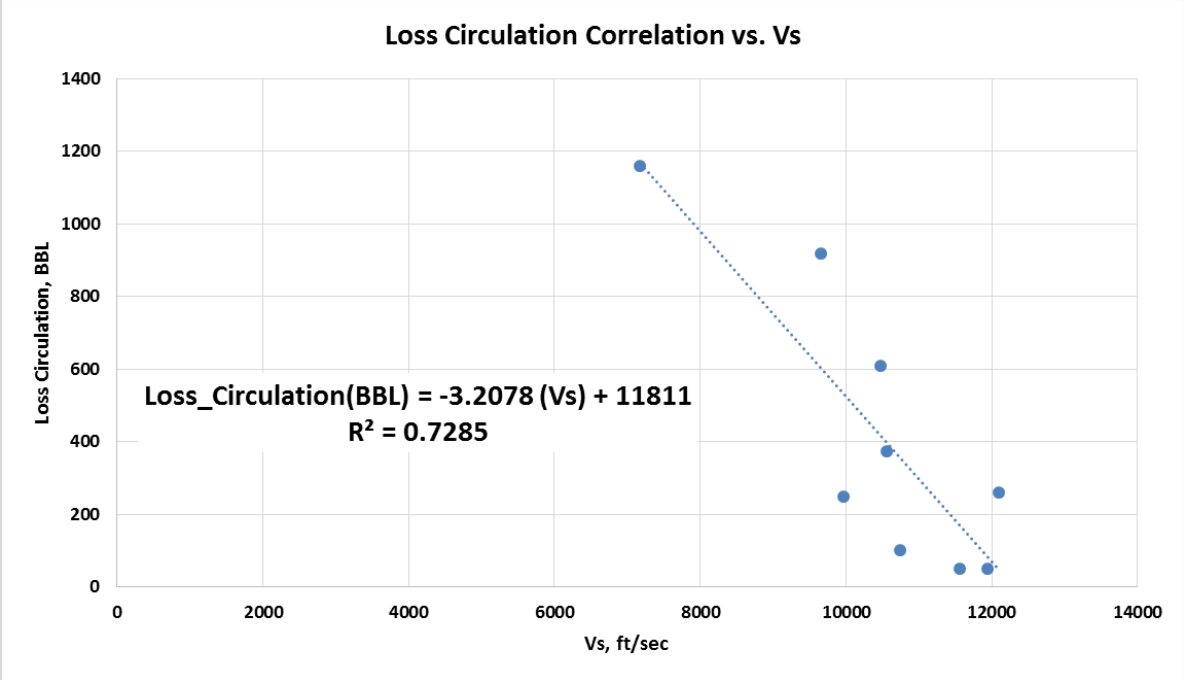

Figure 38: Interpreted cross-plot between loss circulation (BBL) shear velocity Vs (ft./s)

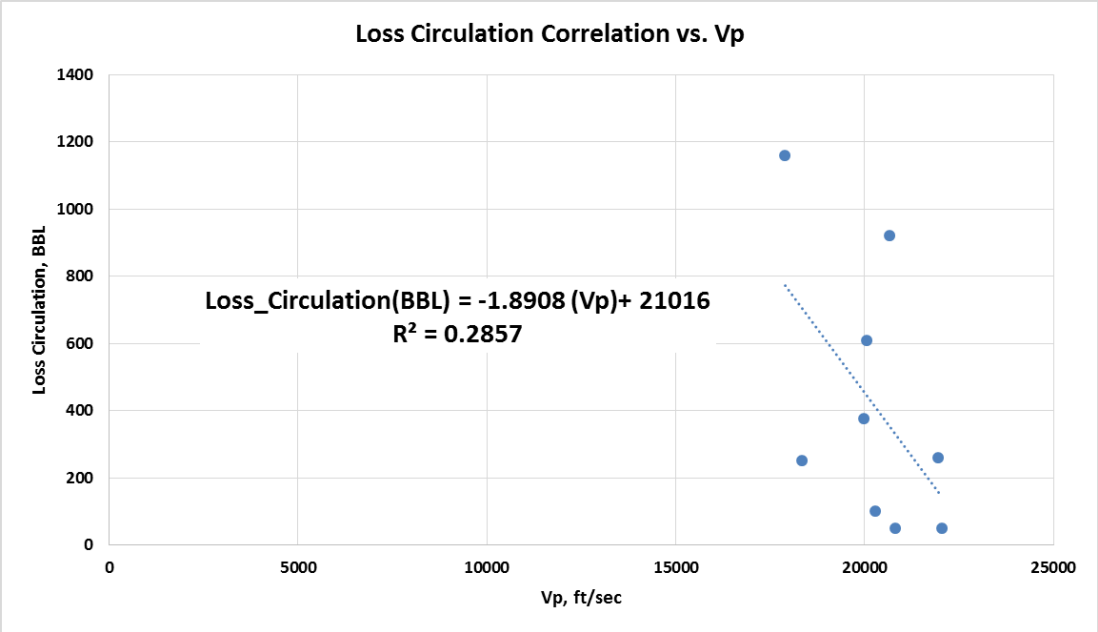

Figure 39: Interpreted cross-plot between loss circulation (BBL) compression velocity Vp (ft./s).

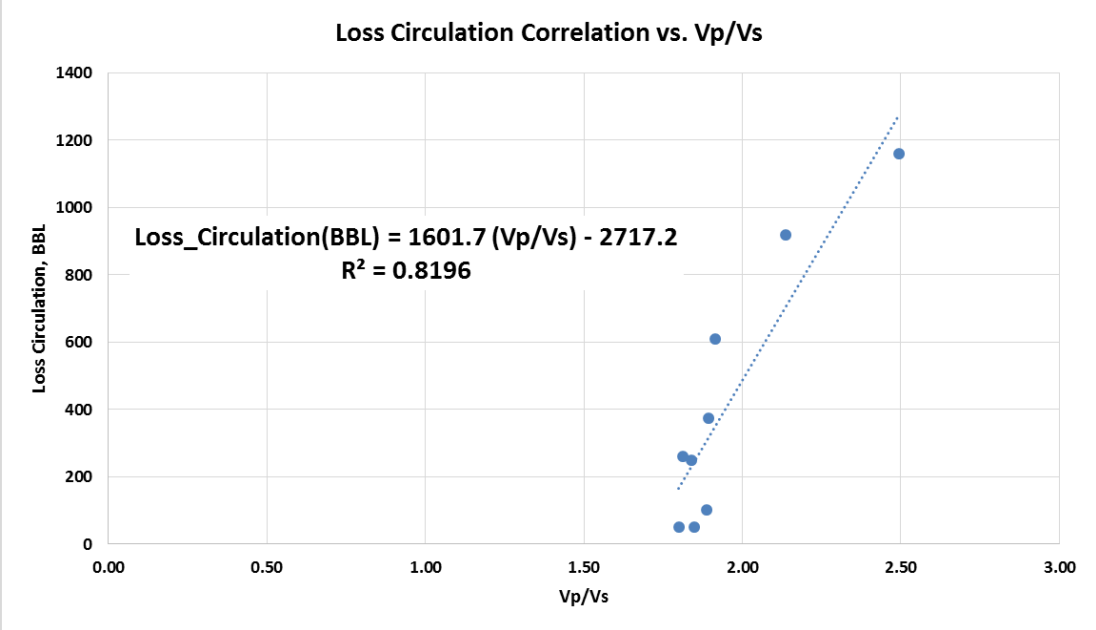

Figure 40: Interpreted cross-plot between loss circulation volume (BBL) and ratio between compression and shear velocities (Vp/Vs).

5.2 Loss Circulation Prediction Using Rock Mechanical Properties

A statistical approach was used to investigate the dependency between loss circulation volume and the rock mechanical properties using the previously introduced correlations in Chapter 6. The rock mechanical properties include Young's Modulus and UCS derived from bulk density data. Values of YM and UCS were estimated at the depth of the loss circulation events using the proposed correlations and the available open hole logs. Both properties were cross-plotted against the loss circulation. A strong relationship between loss gradient in BBL/ft. and the YM was found as shown in Figure 41.

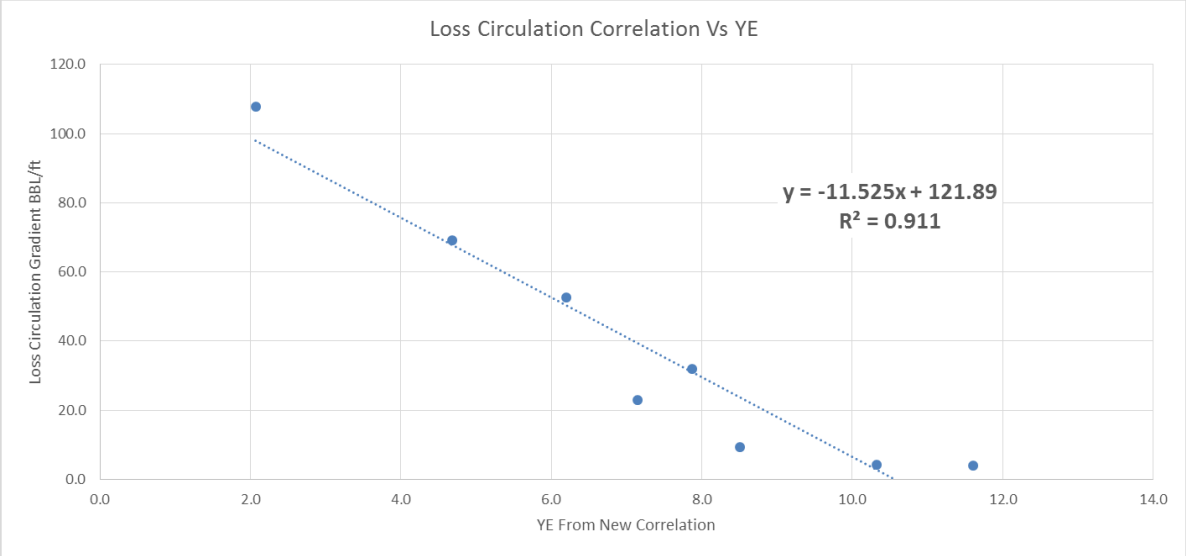

Figure 41: Interpreted cross-plot between loss circulation gradient (BBL/ft.) and YM.

5.3 Observations

The illustrated cross-plots in Figure 37 and Figure 38 shows potential dependency between sonic wave properties (Vp/Vs) and the rock Young's Modulus and the corresponding correlations can be utilized to estimate the likelihood of loss circulations in a particular zone and location in the field. However, to fully confirm the dependency and to provide physical explanation, future core plug testing and modeling will be needed. The advantage of these correlation, once confirmed, will be that using seismic data based Vp/Vs we can build full 3D Seismic volume model for loss circulation which will be constructed using the developed correlation.

CHAPTER 6

CONCLUSION AND RECOMENDATIONS

The motive of this study was to determine the main reasons behind an ever-increasing loss circulation problems in the studied field. The approach used was to analyze the goemechanical data from wells prospective through construction of Mechanical Earth Models to explain the stress acting on the wellbore and understand the loss circulation events. To accomplish that goal, several data streams were collected, analyzed and used in the analysis. Following the analysis, events of loss circulation was classified in view of the safe mud weight window deduced from the MEM model. The existence of natural fractures was also evaluated from image logs. The below summarizes the main findings through the various stages of the investigation:

- The global bulk density extrapolation methods provide the best representation in carbonate reservoirs for estimating the overburden stress. The average error calculated was 5.1 % which is within acceptable range while the maximum error is around 30% compared to 114% using the Amoco method from previous section. Other methods tested had considerable error.
- Modular Dynamic Tester (MDT) provided the best bases for establishing a hydrostatic gradient from which the pore pressure can be estimated.
- The statistical error in estimating YM, UCS and FANG is high utilizing the available literature correlation included in this study and makes further calculation for the MEM unreliable.

- Using core data, the established correlation between dynamic and static Young's Moduli provide better estimation with less error. Also similar correlations were developed for Passion's' ratio, UCS and FANG which gave better estimation than available correlations included in this study.
- Following the qualitative analysis, it was clear that wellbore instability events represented in the loss circulation depths and volumes can be classified into two categories; events where mud weight used exceeded the calculated Safe Mud Weight Window and others that fall within calculated Safe Mud Weight Window.
- For the events where the safe MW window was violated, those can be avoided if a pre-drilling wellbore stability model was used to guide the drilling mud weight design. However, the Image log data confirmed that the depths at which loss circulation occurred although the safe MW window was not violated, do have natural fractures have been observed from the image log data.
- To predict the loss circulation volume, the investigation carried in the study showed potential relationships between the magnitude of loss circulation and the rock mechanic properties such as Young's modulus and the ratio between sonic wave compression and shear velocities. Those findings will help in building predictive full field 3D models which can be optimized for future drilling program in order to minimize loss circulation. However, to confirm the relationships, further lab and simulation work is needed that will be carried in future technical work.

REFRENCES

[1] A., Heinz J. T., Svoboda F. C. et al. “Optimizing the Selection of Bridging Particles for Reservoir Drilling Fluid”. nternational Symposium on Formation Damage Control, 2000.

[2] Abrams, A. 1977. “Mud Design to Minimize Rock Impairment Due to Particle Invasion”. Journal of Petroleum Technology. 29 (5): 586-593.

[3] Ahmed, U., M. Markley and S. Crary "Enhanced In-Situ Stress Profiling With Microfracture Core and Sonic-Logging Data." SPE Formation Evaluation 6 02: 243-251.1991.

[4] Al-Buraik, K. and J. Pasnak "Horizontal drilling in Saudi Arabian oil fields: case histories." Middle East Oil Show.1993.

[5] Awal. M.R., M.A. Mohiuddin " Introducing an Enhanced Calibratio Technique for Core-Log Rock Mechanical Parameters: New Shift Calibratio and Recursive Filtering Techniques". 10th Abu Dhabi International Petroleum Exhibition & Conference (ADIPEC), October 13-16,2005 Abu Dhabi, U.A.E.

[6] Beacom, L.E., H. Nicholson, and R.I. Corfield. "Integratio of Drilling and Geological Data to Understand Wellbore Instability". SPE/IADC Drilling Conference, Amsterdam, The Netherlands, 2001.

[7] Bradely, W.B. "Failure of inclined borehole." J. Energy Resources Technology. Res. 1979.

[8] Bradford, I.D.R., W.A. Aldred, J.M. Cook, E.F.M. Elewaut, J.A. Fuller, T.G. Kristiansen, T.R. Walsgrove. "When Rock Mechanics Met Drilling: Effective Implementation of Real-Time Wellbore Stability Control". IADC/SPE Drilling Conference, New Orleans, 2000.

[9] Bradley, W.B., “Mathematical concept – Stress cloud can predict borehole failure”. Oil and Gas Journal, 1979.

[10] Chang, C., M. D. Zoback and A. Khaksar "Empirical relations between rock strength and physical properties in sedimentary rocks." Journal of petroleum Science and Engineering .2006.

[11] Cheatham Jr, J. "Wellbore stability." Journal of petroleum technology .1984.

[12] Cheng-yuan Xu, Yi-li Kang, Li-jun You, et al. “High-Strength, High-Stability Pill System To Prevent Lost Circulation”. Journal of Petroleum Technology. 2014.

[13] Cui, L., Ekbote, S., & Abousleiman, Y.”Effect of pore fluid conditions at the borehole wall on borehole stability”. American Rock Mechanics Association. 1998.

[14] Fjar, E., R. M. Holt, A. Raaen, R. Risnes and P. Horsrud. "Petroleum related rock mechanics"Elsevier.1992.

[15] Gardner, G. H. F., & Harris, M. H. Velocity And Attenuation Of Elastic Waves In Sands. Society of Petrophysicists and Well-Log Analysts. 1968.

[16] Gatens III, J., C. Harrison III, D. Lancaster and F. Guidry "In-Situ Stress Tests and Acoustic Logs Determine Mechanical Propertries and Stress Profiles in the Devonian Shales." SPE Formation Evaluation.1990.

[17] Goodman, R. E. Introduction to rock mechanics, John Wiley.1980.

[18] Guangzhi, Y., He, Li., & Xuefu, X. "The effect of the stress path on strength of rock". American Rock Mechanics Association. 1988.

[19] Hassan, S., T. Klimentos, M. Badri, M. Sengul and A. Zeid. "Optimizing drilling performance by wellbore stability evaluation and directional drilling practices". SPE/IADC Middle East drilling technology. Symposium.1999.

[20] Hawkes, C., P. McLellan, W. Maurer and C. Ruan "Wellbore instability in shales: a review of fundamental principles and GRI-funded research." GRI Final Report 2000.

[21] Hodge, M. O., Valencia, K. J. L., Chen, Z., & Rahman, S. S. "Analysis of Time-Dependent Wellbore Stability of Underbalanced Wells Using a Fully Coupled Poroelastic Model". Society of Petroleum Engineers. 2006.

[22] Jaeger J.C. and Cook N.G.W., Fundamental of Rock Mechanics, 3rd addition, Chapman and Hall, London UK,1979.

[23] Khaksar, A., P. G. Taylor, Z. Fang, T. J. Kayes, A. Salazar and K. Rahman. "Rock Strength from Core and Logs Where We Stand and Ways to Go". EUROPEC/EAGE Conference and Exhibition, Society of Petroleum Engineers.2009.

[24] Kulander, B. R. et al., "Fractured core analysis: interpretation, logging and use of natural and induced fractures in core", AAPG Methods in Exploratio Series, 1992.

[25] Last, N., Plumb, R.A., Harkness, R., Charlez, P., Alsen, J., McLean, M., "An Integrated Approach to Managing Wellbore Instability in the Cusiana Field, Columbia, South America",1995.

[26] McLean, M. R., & Addis, M. A. "Wellbore Stability: The Effect of Strength Criteria on Mud Weight Recommendations". Society of Petroleum Engineers. 1990.

[27] Morales, R. H., & Marcinew, R. P. "Fracturing of High-Permeability Formations: Mechanical Properties Correlations". Society of Petroleum Engineers. 1993.

[28] N. Morita., G.-F. Fuh., A.D. Black. "Borehole breakdown pressure with drilling fluids—II. Semi-analytical solution to predict borehole breakdown pressure". International Journal of Rock Mechanics and Mining Sciences & Geomechanics. 1999.

[29] Nes, O.-M., Fjær, E., Tronvoll, J., Kristiansen, T. G., & Horsrud, P. "Drilling Time Reduction Through an Integrated Rock Mechanics Analysis". Society of Petroleum Engineers. 2005.

[30] Nguyen, V. X., & Abousleiman, Y. N. “Naturally Fractured Reservoir Three-Dimensional Analytical Modeling: Theory and Case Study”. Society of Petroleum Engineers. 2009.

[31] Onaisi, A., J. Locane and A. Razimbaud. "Stress related wellbore instability problems in deep wells in ABK field". Abu Dhabi International Petroleum Exhibition and Conference, Society of Petroleum Engineers.2000.

[32] Perkins, T. K., & Weingarten, J. S. “Stability and Failure of Spherical Cavities in Unconsolidated Sand and Weakly Consolidated Rock”. Society of Petroleum Engineers. 1988.

[33] Plumb, R., C. Ramshorn and B. Zehner. "Method and apparatus for generatio of 3D graphical borehole analysis", Google Patents.2000.

[34] Plumb, R., Edwards, S., Pidcock, G., Lee, D., & Stacey, B. “The Mechanical Earth Model Concept and Its Application to High-Risk Well Construction Projects”. Society of Petroleum Engineers. 2000.

[35] Plumb, R.A. & Hickman, S.H. “Stress-induced borehole elongation: a comparison between the four-arm dipmeter and the Borehole Televiewer in the Auburn geothermal well” Journal of Geophysical Research, 1985.

[36] Plumb, R.A., “Influence of Composition and Texture on the Failure Properties of Clastic Rocks”, SPE/ISRM 28022, Eurock, 1994

[37] Plumb, R.A., Papanastasiou, P., Last, N., “Constraining the state of stress in tectonically active settings” Eurock, SPE/ISRM,1998.

[38] Rahim, Z. and M. Al-Qahtani "Sensitivity Study on Geomechanical Properties to Determine Their Impact on Fracture Dimensions and Gas Production in the Khuff and Pre-Khuff Formations Using a Layered Reservoir System Approach, Ghawar Reservoir, Saudi Arabia." .2001.

[39] Russell, K. A., C. Ayan, N. Hart, J. Rodriguez, H. Scholey, C. E. Sugden and J. K. Davidson "Predicting and Preventing Wellbore Instability: Tullich Field Development North Sea." SPE Drilling & Completion.2006.

[40] Saidin, S. and S. Smith "Wellbore stability and formation damage consideratios for Bekok field K formation." IADC/SPE Asia Pacific Drilling Technology.2000.

[41] Santarelli, F. J., & Brown, E. T. “Performance of Deep Well Bores In Rock With a Confining Pressure-dependent Elastic Modulus”. International Society for Rock Mechanics.1987.

[42] Santarelli, F. J., Dardeau, C., & Zurdo, C. “ Drilling Through Highly Fractured Formations: A Problem, a Model, and a Cure”. Society of Petroleum Engineers. 1992.

[43] Santarelli, F., D. Dahen, H. Baroudi and K. Sliman. "Mechanisms of borehole instability in heavily fractured rock media". International journal of rock mechanics and mining sciences & geomechanics abstracts, Elsevier.1992.

[44] Santarelli, F., S. Zaho, G. Burrafato, F. Zausa and D. Giacca. "Wellbore stability analysis made easy and practical". IADC/SPE drilling conference.1996.

[45] Schmidt, M.G., Li, X., Steinseik, R., and Ma, T.A., "Numerical model for predicting ultrasonic transducer pulse-echo response to borehole fractures", 33rd Annual Logging Symposium Transactions:Society of Professional Well Log Analysts. 1992.

[46] Sirat, M. ,"Predicting Hydrulic Fracturing in a Carbonate Gas Reservoir in Abu Dhabi Using 1D Mechanical Earth Model: Uncertainty and Constrains. SPE Middle East Unconventional Resources Conference, Muscat Oman. 2015.

[47] Stone, T., Bowen, G., Papanastasiou, P., & Fuller, J. “Fully Coupled Geomechanics in a Commercial Reservoir Simulator”. Society of Petroleum Engineers. 2000.

[48] Timur, A. T. Acoustic Logging (1987 PEH Chapter 51). Society of Petroleum Engineers. 1987

[49] Traugott, M. O. Rock Mechanics, Petrophysics, and Stratigraphy of the Tuscaloosa Trend. Society of Petroleum Engineers. 1982.

[50] Traugott, M., "Pore/fracture pressure determinations in deep water" Deepwater Technology supplement to World Oil, August 1997.

[51] Van oort, E. and Razavi S.R. "Wellbore Strengthening and Casing Smear: The Common Underlying Mechanism". IADC/ SPE Drilling Conference and Exhibition, Worth, Texas,2014.

[52] Van Oort, E., Friedheim, J., Lee, J., et al. "Continuously Strengthening Wellbores Eliminates Lost Circulation". World Oil, 2008.

[53] Van oort, E., Friedheim, J.E., Pierce, T., et al. "Avoiding Losses in Depleted and Weak Zones by Constantly Strengthening Wellbores". SPE Journal of Drilling & Completion. 2011.

[54] Vickers, Stephen R., Hutton, Alistair Paul, Main, Ryan et al. "Drilling Highly Fractured Limestone Reservoirs: Is It a Particle Bridge Too Far?" SPE Annual Technical Conference and Exhibition, Florence, Italy, 2010.

[55] Willson, S. M., Edwards, S., Heppard, P. D., Li, X., Coltrin, G., Chester, D. K., … Cocales, B. W. "Wellbore Stability Challenges in the Deep Water, Gulf of Mexico: Case History Examples from the Pompano Field". Society of Petroleum Engineers. 2003.

[56] Zemanek, J. et al., " The borehole televiewer - a new logging concept for fracture location and other types of borehole inspection" Jouranl of Petroleum Technologies, 1969.

[57] Zhou, S., Hillis, R., & Sandiford, M. "On the Mechanical Stability of lnclined Wellbores" Society of Petroleum Engineers. 1996.

[58] Zoback, M.D, Moos, D., Mastin, L. "Well bore breakouts and in-situ stress". Journal of Geophysical Research, 1985.

[59] Zoback, M.L. et al., "Global patterns of tectonic stress", Nature, 1989.

[60] Zoback, M.L., Reservoir Geomechanics, Version 3, Cambridge University Press 2007.

Vitae

Name:	AbdulRahman Mohammad Al-Nutaifi
Nationality:	Saudi
Date of Birth:	10/29/1987
Email:	abdulrahman.nutaifi@gmail.com
Address	Dhahran, Saudi Arabia

Academic Background:	B.S. in Petroleum Engineering, 2010, King Fahd University of Petroleum & Minerals M.Sc. in Petroleum Engineering, 2019, King Fahd University of Petroleum & Minerals
Work Experience:	Supervisor – Karan, Khursaniyah and Midyan Gas Unit Gas Reservoir Management, Saudi Aramco, (2017-Present). Petroleum Engineering – EXPEC Advanced Research Center, Saudi Aramco, Saudi Arabia (2016-2017). Petroleum Engineering – Gas RMD Technical Unit, Saudi Aramco, Saudi Arabia (2015-2016). Foreman – Gas Completion Operations, Saudi Aramco, Saudi Arabia (2014-2015). Reservoir Engineer – Offshore Gas RMD, Saudi Aramco, Saudi Arabia (2010-2014).

Professional Activities: An active member of SPE (Society of Petroleum Engineers).

2013-2016 Member of organizing committees of SPE Annual Technical Symposium and Exhibition held in Dhahran.

2015- Passed SPGE Petroleum Engineering certification. Certificate of testimony of meeting professional standards and commitment to the profession.

2015- Served as a team member of organization committee of The SPE Gas Well Deliquification workshop.

2016-2017 Served as Vice-Chairman of SPE Membership for Saudi Arabia section.